



## The transformation of Fe(III) oxides catalysed by Fe<sup>2+</sup> and the fate of arsenate during transformation and reduction of Fe(III) oxides

Pedersen, Hanne Dahl

*Publication date:*  
2006

*Document Version*  
Publisher's PDF, also known as Version of record

[Link back to DTU Orbit](#)

*Citation (APA):*  
Pedersen, H. D. (2006). *The transformation of Fe(III) oxides catalysed by Fe<sup>2+</sup> and the fate of arsenate during transformation and reduction of Fe(III) oxides*. DTU Environment.

---

### General rights

Copyright and moral rights for the publications made accessible in the public portal are retained by the authors and/or other copyright owners and it is a condition of accessing publications that users recognise and abide by the legal requirements associated with these rights.

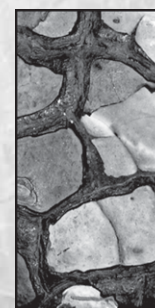
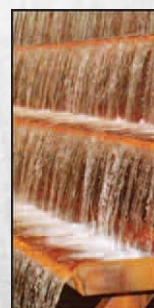
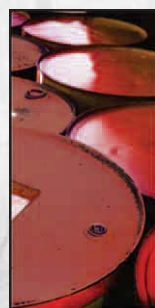
- Users may download and print one copy of any publication from the public portal for the purpose of private study or research.
- You may not further distribute the material or use it for any profit-making activity or commercial gain
- You may freely distribute the URL identifying the publication in the public portal

If you believe that this document breaches copyright please contact us providing details, and we will remove access to the work immediately and investigate your claim.

# The transformation of Fe(III) oxides catalysed by $\text{Fe}^{2+}$ and the fate of arsenate during transformation and reduction of Fe(III) oxides

Hanne Dahl Pedersen

INSTITUTE OF ENVIRONMENT & RESOURCES





**The transformation of Fe(III) oxides catalysed by  
Fe<sup>2+</sup> and the fate of arsenate during  
transformation and reduction of Fe(III) oxides**

**Hanne Dahl Pedersen**

Ph.D. Thesis  
February 2006

Institute of Environment & Resources  
Technical University of Denmark

***The transformation of Fe(III) oxides catalysed by Fe<sup>2+</sup> and the fate of arsenate during transformation and reduction of Fe(III) oxides***

Cover: Torben Dolin & Julie Camilla Middleton  
Printed by: DTU tryk  
Institute of Environment & Resources  
ISBN 87-91855-03-9

The thesis will be available as a pdf-file for downloading from the institute homepage on: [www.er.dtu.dk](http://www.er.dtu.dk)

Institute of Environment & Resources  
Library  
Bygningstorvet, Building 115,  
Technical University of Denmark  
DK-2800 Kgs. Lyngby

**Phone:**

Direct: (+45) 45 25 16 10  
(+45) 45 25 16 00  
Fax: (+45) 45 93 28 50  
E-mail: [library@er.dtu.dk](mailto:library@er.dtu.dk)

## Preface

The present dissertation is submitted as the partial requirement for the attainment of the Ph.D. degree. The research was conducted at the Institute of Environment & Resources at the Technical University of Denmark (DTU), from October 2002 to January 2005. The study was funded by a Ph.D. grant awarded by the Technical University of Denmark and further financed by the Natural Science Research Council. The work has been supervised by Reader Dieke Postma, Associate Professor Rasmus Jakobsen both from the Institute of Environment & Resources, DTU and Dr. Ole Larsen, Ph.D., DHI Water & Environment, Germany.

The dissertation consist of a summary focussing on the transformation of Fe(III) oxides catalysed by Fe<sup>2+</sup> and the fate of arsenate during transformation and reduction of Fe(III) oxides, as well as of two journal papers of which one is published and the other is to be submitted. The in-text references and the titles of the papers are:

Pedersen et al. (2005)

Pedersen, H. D., Postma, D., Jakobsen, R., and Larsen, O. (2005). Fast transformation of iron oxyhydroxides by the catalytic action of aqueous Fe(II). *Geochimica et Cosmochimica Acta*, 69:3967–3977

Pedersen et al. (2006)

Pedersen, H. D., Postma, D., and Jakobsen, R. (2006). Release of arsenic associated with the reduction and transformation of iron oxides. To be submitted to *Geochimica et Cosmochimica Acta*

The papers are not included in this www-version but may be obtained from the Library at the Institute of Environment & Resources, Bygningstorvet, Building 115, Technical University of Denmark, DK-2800 Lyngby (library@er.dtu.dk).

I would like to acknowledge my supervisors Dieke Postma, Rasmus Jakobsen and Ole Larsen for their always careful and fruitful supervision. I would also like to acknowledge Professor Hans Christian Bruun Hansen, the Royal Veterinary and Agricultural University, Denmark for his help and guidance with the XRD measurements. At the Institute of Environment & Resources, DTU, I would like to thank all the people helping me throughout the study, particularly those from the former Department of Geology and Geotechnical Engineering, especially Lene Kirstejn Jensen and Ellen Zimmer Hansen for their assistance in the laboratory, and for the graphical work in this thesis, Torben Dolin. Last, but not least, a special thank to my parents for their everlasting help and support, and to my boyfriend Steffen for his support and the innumerable hours he spend helping with various IT issues during the preparation of this dissertation.

Copenhagen, January 2006

Hanne Dahl Pedersen



## Abstract

Iron oxides are ubiquitous in soils and sediments and have a profound influence on the water chemistry of aquifers and subsurface waters. For example, iron oxides are considered the most important adsorbents for trace metals and arsenic in sandy aquifers because of their great abundance and strong binding affinity. Upon reduction of the iron oxides, the adsorbed species may be released. Furthermore, iron oxides may undergo structural transformations when entering an anoxic environment which may also potentially mobilize the adsorbed species.

The transformation of iron oxides was investigated using the isotopic exchange between aqueous Fe(II) and iron oxides in experiments with  $^{55}\text{Fe}$ -labelled iron oxides.  $^{55}\text{Fe}$  was incorporated congruently into a ferrihydrite, two lepidocrocites (#1 and #2), synthesized at 10°C and 25°C, respectively, a goethite and a hematite. The transformation of the iron oxides was induced by submerging the iron oxides in  $\text{Fe}^{2+}$  solutions (0-1.0 mM) with a pH of 6.5. In the presence of aqueous  $\text{Fe}^{2+}$ , an immediate and very rapid release of  $^{55}\text{Fe}$  was observed from ferrihydrite, the two lepidocrocites and goethite, whereas in the absence of  $\text{Fe}^{2+}$  no release of  $^{55}\text{Fe}$  was observed. Hematite did not release any  $^{55}\text{Fe}$ , even at the higher  $\text{Fe}^{2+}$  concentration. The release rate is mainly controlled by the characteristics of the iron oxides, whereas the concentration of  $\text{Fe}^{2+}$  has only a minor influence.

Within days, ferrihydrite transformed completely into new and more stable phases such as lepidocrocite and goethite at the lower  $\text{Fe}^{2+}$  concentrations and into magnetite at the higher  $\text{Fe}^{2+}$  concentration. No transformation of the other oxides was observed, except for a minor fraction of lepidocrocite that at the higher  $\text{Fe}^{2+}$  concentration transformed into magnetite. For ferrihydrite and 5 nm sized lepidocrocite crystals complete isotopic equilibration with aqueous Fe(II) was attained implying a total disintegration of the original iron oxides. Lepidocrocite #2 and goethite, having larger particles, did not reach isotopic equilibrium within the time frame of the experiment; however, the continuous slow release of  $^{55}\text{Fe}$  suggests that isotopic equilibrium will ultimately be attained.

The fate of trace amounts of arsenate coprecipitated with ferrihydrite, lepidocrocite and goethite was studied during reductive dissolution and phase transformation of the iron oxides using  $^{55}\text{Fe}$  and  $^{73}\text{As}$  labelled iron oxides. The As/Fe molar ratio of the iron oxides ranged from 0 to 0.005 for ferrihydrite and lepidocrocite and from 0 to 0.001 for goethite. All the arsenate remained associated with the surface of ferrihydrite and lepidocrocite whereas only 30% of the arsenate was desorbable from goethite. The rate of reductive dissolution in 10 mM ascorbic acid at pH 3 was unaffected by the presence of arsenate for all of the iron oxides. Arsenate was not reduced to arsenite by the ascorbate and was released incongruently with  $\text{Fe}^{2+}$  for all the iron oxides during the reductive dissolution of the iron oxides. For ferrihydrite and goethite, the arsenate remained adsorbed to the surface and was only released once the surface area became too small to adsorb all the arsenate. In contrast, arsenate preferentially desorbs from the surface of lepidocrocite.

During the  $\text{Fe}^{2+}$  catalysed transformation of ferrihydrite and lepidocrocite, arsenate became bound more strongly to the product phases and was not released to the solution. Arsenate appeared to be preferentially sorbed to the surface of ferrihydrite



and was only incorporated into the crystalline phase at the end of the transformation process. The transformation rate and the transformation products were unaffected by the presence of arsenate at As/Fe molar ratios less than 0.005.

The results presented here imply a recrystallization of solid Fe(III) phases induced by the catalytic action of aqueous Fe(II). Accordingly iron oxides should be considered as dynamic phases that change composition when exposed to variable redox conditions. These results necessitate a re-evaluation of current models for the release of trace metals under reducing conditions, the sequestration of heavy metals by iron oxides and the significance of stable iron isotope signatures. Furthermore, the results show that it may be difficult to predict the release of arsenate during reductive dissolution of iron oxides in natural sediments and that the transformation of the least stable iron oxides into more crystalline Fe(III) oxide phases may be an important trapping mechanism for arsenic in natural sediments. The results are of importance for the understanding of the behaviour of arsenic in aquifers and on sand filters in water works and for the disposal of arsenic containing chemical waste.

## Resumé

Jernoxider er allestedsværende i naturlige miljøer og har stor indflydelse på vandkemi i grundvandsmagasiner og overfladenære vandmiljøer. Eksempelvis betragtes jernoxider som den vigtigste adsorbent for spormetaller og arsen i sandede grundvandsmagasiner på grund af jernoxidernes store udbredelse og evne til at binde kemiske stoffer til overfladen. Ved reduktiv opløsning af jernoxider vil de adsorberede specier frigives til den vandige fase. Adsorberede specier kan ligeledes mobiliseres som følge af strukturelle omdannelser af jernoxiderne til mere stabile faser i anoksiske miljøer.

Transformationen af jernoxider er undersøgt med udgangspunkt i en isotop udveksling mellem opløst Fe(II) og jernoxider mærket med radioaktivt  $^{55}\text{Fe}$ .  $^{55}\text{Fe}$  indbygges homogent i jernoxiderne ferrihydrit, lepidocrocit (#1 og #2), syntetiseret ved henholdsvis  $10^\circ\text{C}$  og  $25^\circ\text{C}$ , goethit og hæmatit. Transformationen af jernoxiderne i opløsninger med  $\text{Fe}^{2+}$  i koncentrationer mellem 0 og 1,0 mM og pH 6,5 er undersøgt. Tilstedeværelsen af opløst  $\text{Fe}^{2+}$  resulterede i en øjeblikkelig og meget hurtig frigivelse af  $^{55}\text{Fe}$  fra ferrihydrit, lepidocrocit (#1 og #2) og goethit, hvorimod en frigivelse af  $^{55}\text{Fe}$  ikke er observeret, når  $\text{Fe}^{2+}$  er fraværende. I forsøgene med hæmatit sker der ingen frigivelse af  $^{55}\text{Fe}$  ved nogen af  $\text{Fe}^{2+}$  koncentrationerne. Hastigheden med hvilken  $^{55}\text{Fe}$  blev frigivet fra jernoxiderne er hovedsagelig relateret til jernoxidernes mineralogiske og fysiske egenskaber, mens selve  $\text{Fe}^{2+}$  koncentrationen kun har mindre betydning.

Ved tilstedeværelsen af  $\text{Fe}^{2+}$  omdannes ferrihydrit fuldstændigt til nye og mere stabile faser såsom lepidocrocit og goethit i løbet af få dage. En tilsvarende omdannelse er ikke observeret for de øvrige jernoxider, bortset fra en mindre del af lepidocrocit, der ved højere  $\text{Fe}^{2+}$  koncentrationer omdannes til magnetit. Ferrihydrit og lepidocrocit med en krystalstørrelse på 5 nm opnåede fuldstændig isotopligevægt med opløst Fe(II), hvilket er i overensstemmelse med en total opløsning af de oprindelige jernoxider. Lepidocrocit #2 og goethit, der havde større krystaller, opnåede ikke isotopligevægt indenfor eksperimenterens varighed, men en fortsat langsom frigivelse af  $^{55}\text{Fe}$  indikerer, at systemet går mod en isotopligevægt.

Ferrihydrit, lepidocrocit og goethit blev udfældet ud fra en opløsning med spormængder af arsenat, og frigivelsen af arsenat under reduktiv opløsning og faseomdannelse af jernoxiderne er undersøgt ved hjælp af såvel radioaktiv  $^{55}\text{Fe}$  som  $^{73}\text{As}$  mærkede jernoxider. Det molære As/Fe-forhold varierede fra 0 til 0,005 for ferrihydrit og lepidocrocit og fra 0 til 0,001 for goethit. På trods af medudfældningen, kunne al arsenat desorberes fra overfladen af ferrihydrit og lepidocrocit, mens arsenat ser ud til, i en vis grad at være indbygget i goethiten, idet kun 30% af arsenaten kunne desorberes herfra. For både ferrihydrit, lepidocrocit og goethit var reduktionshastigheden i 10 mM askorbinsyre ved pH 3 upåvirket af tilstedeværelsen af spormængder af arsenat. Arsenaten blev ikke reduceret til arsenit af askorbat og blev, for alle jernoxiderne, frigivet inkongruent i forhold til  $\text{Fe}^{2+}$  under den reduktive opløsning af jernoxiderne. For ferrihydrit og goethit forblev arsenaten adsorberet til overfladen og blev først frigivet, når jernoxidernes overfladeareal var reduceret tilstrækkeligt til ikke at kunne binde al arsenat. I modsætning hertil blev arsenat frigivet hurtigere fra lepidocrocit end  $\text{Fe}^{2+}$ .

Under  $\text{Fe}^{2+}$  katalyseret transformation af ferrihydrit og lepidocrocit bindes arsenat stærkere til de nye mere krystalline faser og frigives ikke til opløsningen. Arsenat indbygges dog først i de krystalline faser i omdannelsesprocessens slutfase, hvilket er tilskrevet en vedvarende adsorption til den tilbageværende ferrihydrit. Transformationshastigheden og -produktet var upåvirket af tilstedeværelsen af arsenat i molære As/Fe-forhold under 0,005.

De her præsenterede resultater indikerer en rekrystallisering af faste Fe(III) faser forårsaget af en katalytisk effekt af opløst Fe(II). Jernoxider skal derfor opfattes som dynamiske faser, der ændrer sammensætning i miljøer med varierende redox forhold. Resultaterne nødvendiggør en revurdering af nuværende modeller for frigivelsen af sporstoffer under reducerede forhold, tilbageholdelse af tungmetaller ved binding til jernoxider og betydningen af stabile jernisotop fordelinger. Derudover viser resultaterne, at det kan være svært at forudsige frigivelsen af arsenat ved reaktiv opløsning af jernoxider i naturlige miljøer, og at omdannelse af de mindre stabile jernoxider til mere krystalline Fe(III) oxider muligvis er en vigtig mekanisme, der kan immobilisere arsen i naturlig sediment. Resultaterne er blandt andet af betydning for at forstå arsens opførsel i grundvandsmagasiner, på sandfiltre på vandværker samt ved deponering af arsenholdig kemisk affald.

# Contents

<b>1</b>	<b>Introduction</b>	<b>1</b>
1.1	Objectives . . . . .	2
<b>2</b>	<b>Iron oxide minerals</b>	<b>3</b>
2.1	General . . . . .	3
2.2	The crystal structure of the applied iron oxides . . . . .	5
2.2.1	Ferrihydrite . . . . .	5
2.2.2	Lepidocrocite . . . . .	5
2.2.3	Goethite . . . . .	6
2.2.4	Hematite . . . . .	6
2.2.5	Magnetite . . . . .	6
<b>3</b>	<b>Arsenic association with iron oxides</b>	<b>7</b>
3.1	Aqueous speciation . . . . .	7
3.2	Adsorption on iron oxides . . . . .	8
3.2.1	pH dependency . . . . .	8
3.2.2	Maximum sorption densities . . . . .	9
3.2.3	Adsorption mechanism . . . . .	9
3.3	Coprecipitation with iron oxides . . . . .	10
<b>4</b>	<b>Reductive dissolution of iron oxides</b>	<b>13</b>
4.1	Abiotic reductive dissolution . . . . .	13
4.1.1	Fe <sup>2+</sup> catalysed dissolution of Fe(III) oxides . . . . .	14
4.2	Biotic reduction . . . . .	14
4.2.1	Mechanisms of bacterial electron transfer . . . . .	16
4.3	Reactivity . . . . .	16
4.3.1	Rate expression . . . . .	16
4.3.2	Reactivity of iron oxides . . . . .	17
4.3.3	Effect of arsenate on the reactivity of the iron oxides . . . . .	19
4.4	Release of arsenate during reduction of iron oxides . . . . .	20
4.4.1	PHREEQC simulation . . . . .	23
<b>5</b>	<b>Transformation of iron oxides</b>	<b>25</b>
5.1	General . . . . .	25
5.2	Fe <sup>2+</sup> catalysed transformation of Fe(III) oxides . . . . .	25
5.2.1	Mechanism for Fe <sup>2+</sup> catalysed transformation of Fe(III) oxides . . . . .	29
5.2.2	Kinetics of Fe(III) oxide transformation . . . . .	31
5.2.3	Effect of adsorbed arsenate on the transformation of Fe(III) oxides . . . . .	33
5.3	The fate of adsorbed arsenate . . . . .	35
<b>6</b>	<b>Discussion</b>	<b>39</b>
6.1	Fe <sup>2+</sup> catalysed transformation of Fe(III) oxides . . . . .	39
6.2	The fate of arsenic . . . . .	41
<b>7</b>	<b>Conclusions</b>	<b>43</b>
	<b>References</b>	<b>45</b>



# 1 Introduction

Iron oxides are a group of minerals widespread in nature. In ancient time, they were used by man to produce prehistoric paintings in caves and since then the use of iron oxides has expanded enormously. Presently, iron oxides are, among many other fields, still used as pigments in paint, but now also as catalysts in various chemical reactions and as precursors for iron and steel.

In natural soil and sediments, iron oxides are omnipresent and have a profound influence on the water chemistry of aquifers and sub-surface waters. Due to their high specific surface area, iron oxides act as important sorbents for dissolved species, for example heavy metals, phosphate and arsenate (Rozan et al., 2002; Appelo and Postma, 2005), and thereby control the aqueous concentration of these species. Furthermore, under reducing conditions, the iron oxides may be reductively dissolved while releasing  $\text{Fe}^{2+}$  and in many subsurface environments Fe(III) is the most abundant of the available terminal electron acceptors for the oxidation of organic matter. For example, many deep pristine aquifers have extensive anaerobic zones in which organic matter is oxidized with the reduction of Fe(III) (Lovley, 1997). Also in shallow aquifers, although aerobic in their pristine state, anaerobic plumes with an extensive zone of Fe(III) reduction can develop if these aquifers are contaminated with organic compounds such as petroleum products or landfill leachate (Albrechtsen and Christensen, 1994). The reduction of iron oxides by organic matter may occur directly or, more often, mediated by micro-organisms using the organic matter as substrate (Lovley et al., 1991; Albrechtsen and Christensen, 1994; Lovley, 1997). In marine environments also the reduction of iron oxides by sulphide may be of importance (Canfield et al., 1992; dos Santos Afonso and Stumm, 1992; Yao and Millero, 1996).

Natural iron oxides comprise a mix of a range of minerals, most commonly ferrihydrite, lepidocrocite, goethite and hematite, with different characteristics such as stability, specific surface area and reactivity (Larsen and Postma, 2001; Cornell and Schwertmann, 2003). The formation and persistence of the more unstable oxides is due to kinetic inhibition in the transformation to more stable phases. Laboratory experiments have shown that the association of iron oxides with aqueous  $\text{Fe}^{2+}$ , either biologically produced or added as  $\text{FeCl}_2$  may promote the transformation of the least stable iron oxides, most often ferrihydrite, to more stable phases, such as hematite and goethite (Fischer, 1972; Hansel et al., 2003; Jang et al., 2003; Jeon et al., 2003), or to mixed valence compounds such as green rust or magnetite (Tamura et al., 1983; Tronc et al., 1992; Jolivet et al., 1992; Ona-Nguema et al., 2002).

Upon reduction and phase transformation of the iron oxides, the available surface area decreases and the adsorbed species may potentially be released. One of the hypothesis for the serious problems with arsenic contaminated groundwaters in many areas of the world, is that the arsenic, originally adsorbed to the iron oxides, is released as a consequence of the reductive dissolution of iron oxides (Nickson et al., 2000; McArthur et al., 2001; Schwartz et al., 2004; Tareq et al., 2004). Well-known areas with groundwater containing arsenic in concentrations that may by far exceed the WHO guideline of  $10 \mu\text{g/L}$  include West Bengal (India), Bangladesh, Vietnam, Argentina and China (Smedley and Kinniburgh, 2002). As arsenic is known to be carcinogenic, the high concentration of arsenic in the drinking water constitute a

serious health problem in the affected areas.

The exact mechanisms causing the release of arsenic to the groundwaters in the Bengal Basin are not known, although there is general consensus that the arsenic stems from natural sediment-water interaction. Beside reductive dissolution of iron oxides, also oxidation of arsenic containing pyrite (Das et al., 1996; Mandal et al., 1998), reduction of adsorbed arsenate to arsenite on the mineral surfaces (Kiniburgh and Smedley, 2001; Bose and Sharma, 2002), competitive anion exchange of adsorbed arsenic (Acharyya et al., 1999; Appelo et al., 2002) has been proposed.

Since the discovery of radioactivity by A. H. Becquerel in 1896, the use of radio tracers has gained appreciation within several scientific fields, the most well-known being medicine and archaeology. Radioactivity is the result of changes within the nuclei of radioactive isotopes i.e. unstable atomic nuclei containing the same number of protons but varying numbers of neutrons. The changes comprise an adjustment of the neutron-to-proton ratio to stabilize the nucleus and are accompanied by spontaneous emission of particles and/or electromagnetic radiation from the nucleus. Since, in general, the chemical behaviour of an atom depends only on the properties of the atomic electrons, and different isotopes of the same element have the same electronic structure for their atoms, the isotopes are believed to behave chemically identically. This makes radioactive isotopes ideal as tracers in studies of the kinetics and mechanisms of chemical processes since the radio tracers are easily detected due to the radiation emitted during decay. To mention a few examples, radio tracers have been used to study the sorption of divalent metals on calcite (Zachara et al., 1991), the sorption of pesticides onto minerals surfaces (Clausen et al., 2001), the pathway for metal movement in plants (Jackson, 1998), the isotopic exchange between Fe(III) and Fe(II) during precipitation of  $^{55}\text{Fe(III)}$  as ferrihydrite in the presence of  $\text{Fe}^{2+}$  (Roden and Lovley, 1993), and the pathway for methane production (Hansen et al., 2001). Radio tracer rate measurements of the sulphate reduction rate (Jørgensen, 1978; Ferdelman et al., 1997; Jakobsen and Postma, 1999; Hansen et al., 2001) and methane production rate (Hansen et al., 2001) in natural sediments are also widely applied.

## 1.1 Objectives

The objectives of this study are to use radio tracers to investigate

- The catalytic action of  $\text{Fe}^{2+}$  on the transformation of ferrihydrite, lepidocrocite, goethite and hematite.
- The effect of trace amounts of arsenate on the transformation of ferrihydrite and lepidocrocite.
- The fate of arsenate during reductive dissolution and transformation of iron oxides.

## 2 Iron oxide minerals

### 2.1 General

Iron oxides are a group of minerals composed of Fe together with O and/or OH. In reality they consist of either oxides, hydroxides or oxide-hydroxides but are throughout this thesis collectively referred to as iron oxides. Some characteristic features of iron oxides include low solubility, and thereby high stability, conspicuous colours, and high surface area making them very effective sorbents for a number of dissolved species. There are 17 known iron oxides (Table 1) differing in the composition, valence of Fe and most importantly in the crystal structure. Most of the iron oxides contain Fe(III); only in FeO and Fe(OH)<sub>2</sub> is iron exclusively present in the divalent state, while green rusts and magnetite are mixed Fe(II)-Fe(III) minerals. There are five polymorphs of FeOOH and four of Fe<sub>2</sub>O<sub>3</sub>. Nearly all the iron oxides are crystalline, with the exception of ferrihydrite and schwertmannite which are poorly crystalline. The degree of crystal order is, however, variable and depends on the conditions under which the iron oxides are formed (Cornell and Schwertmann, 2003).

Table 1: Overview of iron oxides (Cornell and Schwertmann, 2003)

Oxides–hydroxides and hydroxides		Oxides	
Goethite	$\alpha$ -FeOOH	Hematite	$\alpha$ -Fe <sub>2</sub> O <sub>3</sub>
Lepidocrocite	$\gamma$ -FeOOH	Magnetite	Fe <sub>3</sub> O <sub>4</sub> (Fe <sup>II</sup> Fe <sub>2</sub> <sup>III</sup> O <sub>4</sub> )
Akaganeite	$\beta$ -FeOOH	Maghemite	$\gamma$ -Fe <sub>2</sub> O <sub>3</sub>
Schwertmannite	Fe <sub>16</sub> O <sub>16</sub> (OH) <sub>y</sub> (SO <sub>4</sub> ) <sub>z</sub> · nH <sub>2</sub> O	–	$\beta$ -Fe <sub>2</sub> O <sub>3</sub>
–	$\delta$ -FeOOH	–	$\epsilon$ -Fe <sub>2</sub> O <sub>3</sub>
Feroxyhyte	$\delta'$ -FeOOH	Wüstite	FeO
High pressure	FeOOH		
Ferrihydrite	Fe <sub>5</sub> HO <sub>8</sub> · 4H <sub>2</sub> O		
Bernalite	Fe(OH) <sub>3</sub>		
–	Fe(OH) <sub>2</sub>		
Green Rusts	Fe <sub>x</sub> <sup>III</sup> Fe <sub>y</sub> <sup>II</sup> (OH) <sub>3x+2y-z</sub> (A <sup>-</sup> ) <sub>z</sub> ; A <sup>-</sup> = Cl <sup>-</sup> ; 1/2 SO <sub>4</sub> <sup>2-</sup>		

In general the stability of iron oxides is high with solubility products ( $[\text{Fe}^{3+}][\text{OH}^{-}]^3$ ) ranging from  $10^{-44}$  to  $10^{-34}$  (Cornell and Schwertmann, 2003). Hence, in natural environments, Fe(III) is mostly found as solid phase Fe(III), and in the pH range 4 to 10, and in the absence of complexing agents, the concentration of Fe(III) is less than  $10^{-6}$  M (Cornell and Schwertmann, 2003). The most unstable form is ferrihydrite while the most stable phases are goethite and hematite. The occurrence of the less stable iron oxides reflects the slow formation kinetics of the more stable phases.

Iron oxides consist of arrays of iron and oxygen or hydroxides. Since the oxygens and hydroxides are much larger than the iron atoms, the crystal structure of the oxides is controlled by the arrangement of the oxygens and hydroxides. The sheets of oxygen and hydroxide are most commonly stacked ABAB... (hexagonal close packing, abbreviated hcp) or ABCABC... (cubic close packing, condensed ccp)



while Fe is placed in the interstices between the oxygen and hydroxide sheets. To fulfil the charge balance requirement, only part of the interstices is filled with Fe. The various iron oxides differ in the arrangement of Fe in the interstices, and to a lesser extent differences in the stacking of the oxygen and hydroxide sheets.

Fe is predominantly octahedrally ( $\text{FeO}_6$  or  $\text{FeO}_3(\text{OH})_3$ ) and in some cases tetrahedrally ( $\text{FeO}_4$ ) coordinated in the iron oxides and the resultant octahedra and tetrahedra constitute the basic structural unit of iron oxides. An alternative way of considering the iron oxide crystal structure is the linkage of these basic structural units since the linkage by sharing either corners, edges or faces results in different iron oxides.

A number of cations other than Fe such as Mn, Al, or Ni have been found to occupy the interstices of iron oxides. The likelihood of substitution depends on the similarity of the ionic radii and the valence of the cations with the most suitable cations being trivalent with an ionic radius between 0.053 - 0.076 nm (Cornell and Schwertmann, 2003). Di- and tetravalent cations may also substitute for Fe in the iron oxide structure, but uptake of these valences is usually less than 10%.

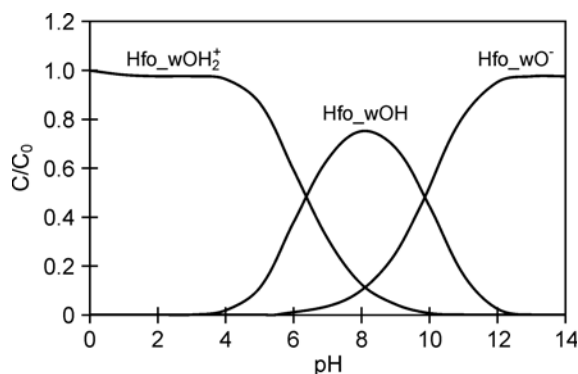


Figure 1: The surface speciation of ferrihydrite as a function of pH as calculated with PHREEQC (Parkhurst and Appelo, 1999).

Figure 1 shows the pH dependence of surface speciation of ferrihydrite in pure water as calculated with PHREEQC (Parkhurst and Appelo, 1999) based on the model of Dzombak and Morel (1990). In acidic environments the oxide surface is positively charged while in alkaline media it is negatively charged. The pH at which the net surface charge is zero is termed the point of zero charge (PZC). Pure iron oxides without sorbing ions have PZC's ranging from 8.5 to 9.3 (Cornell and Schwertmann, 2003). However, adsorption of anions may shift the PZC to lower pH values, while adsorption of cations may shift the PZC to higher pH (Goldberg and Johnston, 2001; Cornell and Schwertmann, 2003).

## 2.2 The crystal structure of the applied iron oxides

### 2.2.1 Ferrihydrite

Ferrihydrite is a reddish brown iron oxide widespread in nature and is often termed "amorphous iron oxide" or "hydrous ferric oxide (HFO)". The composition is variable, a preliminary formula often used is  $\text{Fe}_5\text{O}_8\text{H}\cdot\text{H}_2\text{O}$ . Ferrihydrite is generally poorly ordered. The degree of ordering is indicated by the XRD pattern where the number of reflections increases from 2 to 6-8 as structural order increases. The two end-members are termed 2-line and 6-line ferrihydrite. Ferrihydrite is the least stable iron oxide and it transforms with time into more stable iron oxides and is thus an important precursor for iron oxides of higher crystallinity. The morphology of ferrihydrite is spherical and unlike other iron oxides it exists only as nano crystals resulting in high specific surface areas ranging from 100 - 700  $\text{m}^2/\text{g}$  (Jambor and Dutrizac, 1998; Cornell and Schwertmann, 2003) depending on the method used to measure the surface area. The structure of ferrihydrite is still under debate as the low degree of order impedes the elucidation of the structure (Drits et al., 1993; Waychunas et al., 1996; Jambor and Dutrizac, 1998; Janney et al., 2000).

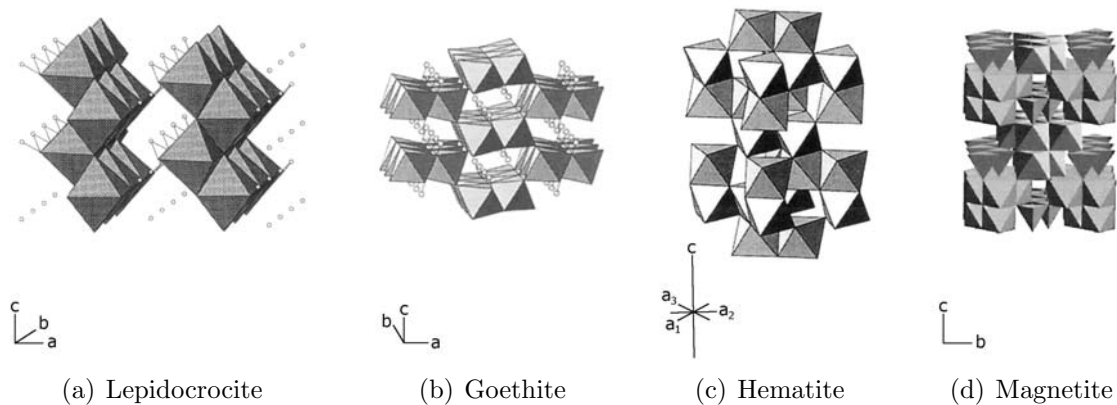


Figure 2: The structure of lepidocrocite, goethite, hematite and magnetite (Cornell and Schwertmann, 2003) With permission from WILEY-VCH Verlag.

### 2.2.2 Lepidocrocite

Lepidocrocite ( $\gamma\text{-FeOOH}$ ) is an orange iron oxide and a common oxidation product of  $\text{Fe}^{2+}$ . The structure of lepidocrocite consists of double chains of edge sharing octahedra running along the  $c$ -axis (Fig. 2). The double chains are linked to adjacent chains by edge sharing, with one chain being displaced by half an octahedral with respect to its neighbour thereby creating corrugated sheets of octahedra. The basic morphologies of lepidocrocite are lath-like or tabular and the specific surface area range from 15 - 260  $\text{m}^2/\text{g}$  (Cornell and Schwertmann, 2003).

### 2.2.3 Goethite

Goethite ( $\alpha$ -FeOOH) is yellow suspended as particles in aqueous solutions and is one of the thermodynamically most stable iron oxides at ambient temperature. Similar to lepidocrocite, goethite is composed of double chains of edge sharing octahedra, but in goethite the octahedra are rotated and the double chains linked by corner sharing and displaced by half a unit cell along the b-axis with respect to its neighbour (Fig. 2). The apparent tunnels in the goethite structure in Figure 2 are not true tunnels but empty octahedral sites. Although goethite displays a range of shapes, the basic morphology is acicular. The specific surface area range from 8 - 200 m<sup>2</sup>/g (Cornell and Schwertmann, 2003).

### 2.2.4 Hematite

Hematite ( $\alpha$ -Fe<sub>2</sub>O<sub>3</sub>) is a blood red iron oxide found widespread in rocks and soils. Like goethite, hematite is very stable. Hematite consists of octahedra sharing edges with three adjacent octahedra in the same plane and one face with an octahedron in a neighbouring plane (Fig. 2). The specific surface area ranges from 10 - 90 m<sup>2</sup>/g and the most common habits for hematite crystals are rhombohedral, platy and rounded (Cornell and Schwertmann, 2003).

### 2.2.5 Magnetite

Magnetite (Fe<sub>3</sub>O<sub>4</sub>) is a black, ferromagnetic mineral containing both Fe(II) and Fe(III). The structure consists of octahedral and mixed octahedral/tetrahedral layers packed along [111] (Fig. 2). In stoichiometric magnetite Fe(II)/Fe(III) = 0.5 but magnetite is often non-stoichiometric resulting in a cation deficient Fe(III) layer. The crystal forms of magnetite include octahedron and rhombodecahedron and the specific surface area ranges from 4 - 100 m<sup>2</sup>/g (Cornell and Schwertmann, 2003).

### 3 Arsenic association with iron oxides

#### 3.1 Aqueous speciation

Arsenic may occur in the environment in the -3, 0, +3 and +5 oxidation states. In natural waters soluble arsenic is found in inorganic form as oxyanions of trivalent arsenic, termed arsenite (As(III)) or pentavalent arsenic, named arsenate (As(V)) (Smedley and Kinniburgh, 2002; Viraraghavan et al., 1999). In the presence of the appropriate micro-organisms, methylation of arsenic oxyanions can occur, forming organic arsenic species. Organic arsenic compounds are, however, quantitatively insignificant (Viraraghavan et al., 1999). Typical concentrations of arsenic in freshwater are frequently less than  $1 \mu\text{g/l}$ , however, values as high as  $5000 \mu\text{g/l}$  have been reported (Smedley and Kinniburgh, 2002).

The most important factors controlling the speciation of arsenate and arsenite are the redox potential and the pH. In oxidized environments arsenate species predominate whereas under reducing conditions arsenite is dominant. However, both oxidation states are often found in soil and subsurface environments regardless of the redox conditions due to the relatively slow kinetics of arsenic redox transformations (Masscheleyn et al., 1991).

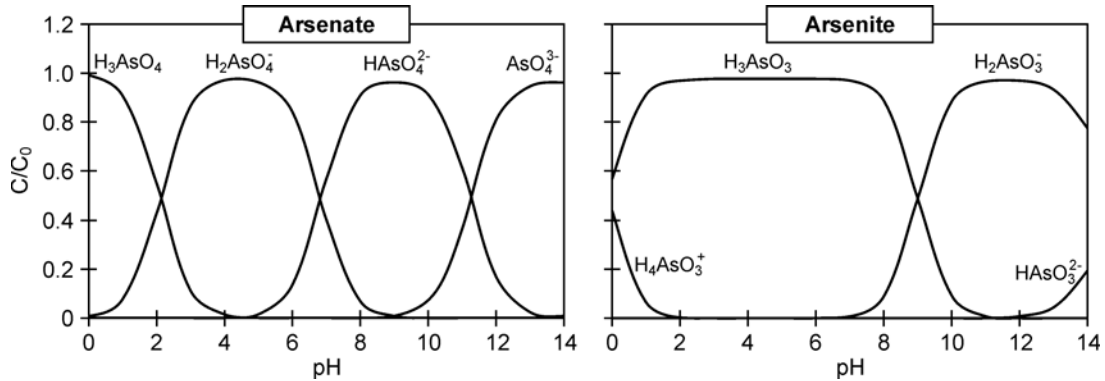


Figure 3: Aqueous speciation of arsenic at various pH values as calculated with PHREEQC (Parkhurst and Appelo, 1999).

Arsenate occurs as arsenic acid ( $\text{H}_3\text{AsO}_4$ ) while arsenite occurs as arsenious acid ( $\text{H}_3\text{AsO}_3$ ) and both arsenate and arsenite form protolytes which may release protons stepwise at increasing pH. The predominating arsenate and arsenite species at various pH values as calculated with PHREEQC (Parkhurst and Appelo, 1999) is shown in Figure 3. The most abundant arsenate species in groundwater are  $\text{H}_2\text{AsO}_4^-$  and  $\text{HAsO}_4^{2-}$  with the former predominating at pH less than 6.76 and the latter at higher pH. In extremely acidic and alkaline environments  $\text{H}_3\text{AsO}_4$  and  $\text{AsO}_4^{3-}$ , respectively may prevail. For arsenite, the uncharged species  $\text{H}_3\text{AsO}_3$  will predominate at pH less than about pH 9.15, whereas  $\text{H}_2\text{AsO}_3^-$  becomes dominant at higher pH.

## 3.2 Adsorption on iron oxides

Due to their large surface areas iron oxides are considered as one of the most important adsorbents regulating the concentration of arsenic in natural waters and numerous studies have been conducted to investigate the adsorption of arsenic to iron oxide surfaces. Both arsenate and arsenite have strong affinities for the iron oxide surface (Pierce and Moore, 1982; Fuller et al., 1993; Waychunas et al., 1993, 1995a; Sun and Doner, 1996; Grossl et al., 1997; Manning et al., 1998; Raven et al., 1998; Jain et al., 1999). Though thermodynamically possible, the oxidation of arsenite by structural Fe(III) upon adsorption onto the iron oxides has not been observed (Manning et al., 1998; Goldberg, 2002; Farquhar et al., 2002).

### 3.2.1 pH dependency

Figure 4 shows the adsorption of arsenate and arsenite on ferrihydrite as calculated with PHREEQC (Parkhurst and Appelo, 1999) based on the Dzombak and Morel (1990) model. Similar results have been found experimentally for both ferrihydrite and goethite (Pierce and Moore, 1982; Hsai et al., 1994; Raven et al., 1998; Goldberg, 2002; Dixit and Hering, 2003). Arsenate adsorption is characterized by an adsorption maximum at acidic pH values and decreasing adsorption with increasing pH above approximately pH 9. The lower adsorption of arsenate at high pH values is attributable to an increased repulsion between the more negatively charged arsenate species (Fig. 3) and negatively charged surface sites (Fig. 1) (Raven et al., 1998).

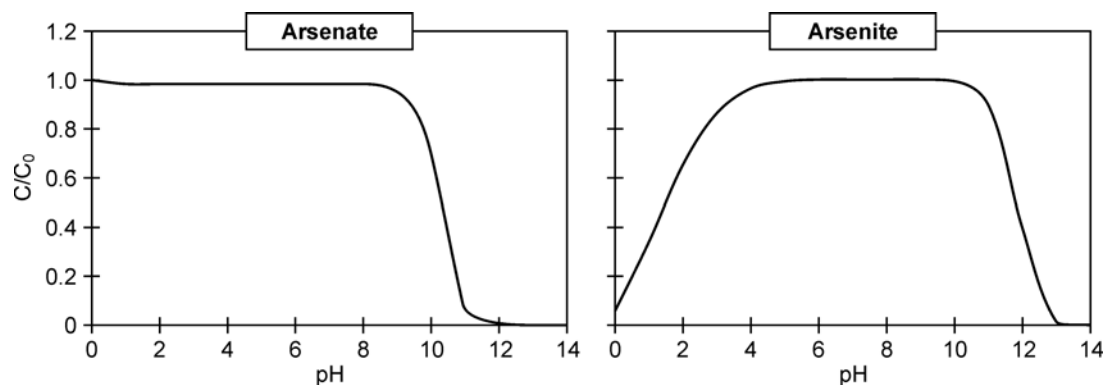


Figure 4: Adsorption of arsenate and arsenite on ferrihydrite at various pH values as calculated with PHREEQC (Parkhurst and Appelo, 1999) using a specific surface area of  $600 \text{ m}^2/\text{g}$  and a concentration of  $1 \text{ mM}$  of iron oxide and a arsenate/arsenite concentration of  $0.133 \text{ } \mu\text{mol/L}$  ( $10 \text{ } \mu\text{g/L}$ ).

Compared to arsenate, the effect of pH on sorption of arsenite is much less pronounced in the pH range of most natural systems (Fig. 4). Sorption of arsenite increases with increasing pH until a broad sorption maximum is observed after which sorption decreases with further increases in pH (Pierce and Moore, 1982; Hsai et al., 1994; Manning et al., 1998; Raven et al., 1998; Goldberg, 2002; Dixit and Hering, 2003). Since arsenite carry less negative charge as compared to arsenate species at the same pH value, they do not exhibit as much repulsion, and as a result, the adsorption decreases less with increasing pH (Raven et al., 1998).

The difference in the pH dependency of arsenate and arsenite adsorption implies that arsenate sorption is more favourable than that of arsenite at lower pH whereas the opposite is the case at neutral to alkaline pH values. The pH at which arsenate and arsenite are equally sorbed depends on the iron oxide, on the arsenic concentration and on the concentration of other ions in the system (Sun and Doner, 1996; Manning et al., 1998; Dixit and Hering, 2003; Raven et al., 1998).

### 3.2.2 Maximum sorption densities

Raven et al. (1998) reported sorption maxima for arsenate on ferrihydrite corresponding to 0.25 and 0.16 mol As/mol Fe at pH 4.6 and 9.2, respectively. In accordance herewith, Dixit and Hering (2003) found a sorption density of 0.24 mol As/mol Fe at pH 4, while a sorption density of 0.25 mol As/mol Fe at pH 8 was reported by Fuller et al. (1993). For arsenite, there are substantial discrepancies in estimates of the maximum sorption density on ferrihydrite, and sorption densities of 0.31 mol As/mol Fe (Dixit and Hering, 2003), 0.6 mol As/mol Fe (Raven et al., 1998), and 0.046 and 5 mol As/mol Fe at low and high arsenic concentration, respectively (Pierce and Moore, 1982), have been reported. The biphasic behaviour with very high sorption densities at high arsenic concentrations was reported for both arsenate and arsenite sorption on ferrihydrite (Pierce and Moore, 1982). However, since sorption of a species must be limited by the availability of surface sites (0.25 mol/mol Fe (Dzombak and Morel, 1990)) it is questionable whether a sorption density of 5 mol As/mol Fe is consistent with pure sorption process.

For goethite, a maximum sorption of 0.016 mol As/mol Fe for both arsenate and arsenite has been reported, while the maximum sorption density of arsenite on magnetite is 2.2 mol As/mol Fe (Dixit and Hering, 2003). The higher maximum sorption densities of arsenate on ferrihydrite as compared to goethite are consistent with similar densities of sorption sites per unit area for the two iron oxides (2.6 and 2.0 sites/nm<sup>2</sup> for ferrihydrite and goethite, respectively) (Dixit and Hering, 2003) in combination with the difference in specific surface area. However, intrinsic surface complexation constants for arsenate are higher for goethite than ferrihydrite, whereas arsenite binding is similar for both ferrihydrite, goethite and magnetite (Dixit and Hering, 2003).

### 3.2.3 Adsorption mechanism

Spectroscopic studies (Waychunas et al., 1993; Hsai et al., 1994; Sun and Doner, 1996; Fendorf et al., 1997; Goldberg and Johnston, 2001; Farquhar et al., 2002), pressure-jump relaxation kinetics measurements (Grossl and Sparks, 1995; Grossl et al., 1997) and titration measurements (Hsai et al., 1994; Jain et al., 1999) show that arsenate adsorbs to iron oxides by forming inner-sphere surface complexes by ligand exchange with hydroxyl groups at the mineral surface. Arsenite has been found to form both inner-sphere (Sun and Doner, 1996; Manning et al., 1998; Goldberg and Johnston, 2001; Farquhar et al., 2002) and outer-sphere (Goldberg and Johnston, 2001) surface complexes on iron oxides.

Though there is general consensus that arsenate forms inner-sphere surface complexes on the surface of iron oxides, the exact nature of the arsenate surface com-

plexes remains controversial. The proposed surface complexes are shown in Figure 5 and include bidentate complexes resulting from corner-sharing between  $\text{AsO}_4$  tetrahedra and edge-sharing pairs of  $\text{FeO}_6$  octahedra (designated  ${}^2\text{C}$  in Fig. 5) (Waychunas et al., 1993; Manceau, 1995; Sun and Doner, 1996; Fendorf et al., 1997; Randall et al., 2001; Farquhar et al., 2002; Sherman and Randall, 2003), bidentate edge-sharing between arsenate tetrahedra and free  $\text{FeO}_6$  edges ( ${}^2\text{E}$  in Fig. 5) (Manceau, 1995; Fendorf et al., 1997; Farquhar et al., 2002) and monodentate complexes resulting from corner sharing between  $\text{AsO}_4$  tetrahedra and  $\text{FeO}_6$  octahedra ( ${}^1\text{V}$  in Fig. 5) (Fuller et al., 1993; Waychunas et al., 1993; Manceau, 1995; Fendorf et al., 1997; Jain et al., 1999).

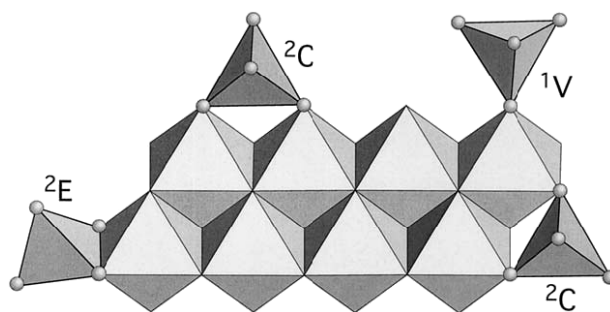


Figure 5: Possible surface complexes of arsenate tetrahedra on iron oxides (Sherman and Randall, 2003) With permission from Elsevier.

Several authors have found the co-existence of two or all three of the proposed surface complexes. The existence of the bidentate binuclear ( ${}^2\text{C}$ ) surface complex is widely accepted whereas the existence of the bidentate mononuclear ( ${}^2\text{E}$ ) and the monodentate ( ${}^1\text{V}$ ) surface complexes is more controversial (Waychunas et al., 1993, 1996; Manceau, 1995). Fendorf et al. (1997) proposed that the relative importance of each surface complex depends on the degree of surface loading with the monodentate surface complex being favoured at low surface coverage and the bidentate surface complexes especially the bidentate, binuclear surface complex being more prevalent at higher surface coverages.

Arsenite appears to associate with the iron oxide surface through a bidentate, binuclear surface complex (Farquhar et al., 2002; Manning et al., 1998; Sun and Doner, 1996).

### 3.3 Coprecipitation with iron oxides

Identical sorption densities have been found for arsenite adsorption and coprecipitation with ferrihydrite (Raven et al., 1998) whereas significantly greater sorption densities have been found for arsenate coprecipitated with ferrihydrite (0.7 mol As/mol Fe) as compared to post-synthesis adsorption (0.25 mol As/mol Fe) (Fuller et al., 1993; Waychunas et al., 1995a; Raven et al., 1998). However, in adsorption experiments, the initial fast adsorption of arsenate was followed by a continued uptake due to diffusion of arsenate to adsorption sites on ferrihydrite surfaces within aggregates of colloidal particles, whereas a release of arsenate was observed upon ageing in

coprecipitation experiments due to crystallite growth, and the two systems appeared to converge to similar steady state concentrations (Fuller et al., 1993).

Despite the high sorption densities, the precipitation of an arsenic oxide, of a ferric arsenate surface phase or the formation of a solid solution has not been observed during the precipitation of ferrihydrite in the presence of arsenate (Waychunas et al., 1993; Rancourt et al., 2001; Richmond et al., 2004). Instead arsenate is adsorbed onto the ferrihydrite surface (Fuller et al., 1993; Waychunas et al., 1993, 1996; Rancourt et al., 2001; Richmond et al., 2004; Pedersen et al., 2006). In this study, aging of a ferrihydrite precipitated in the presence of arsenate in the molar ratio of 0.001, for up to four weeks revealed that the arsenate remains adsorbed on to the surface of ferrihydrite and does not diffuse into the deeper parts of the ferrihydrite particles, since all the arsenate was easily desorbable after four weeks of aging (Pedersen et al., 2006).

The high sorption densities of ferrihydrite precipitated in the presence of arsenate arises from rapid adsorption of arsenate onto the primary ferrihydrite nuclei as soon as these appear in precipitates, leading to increased structural disorder and retardation of crystal growth and aggregation by preventing further Fe-O-Fe-polymerization (Fuller et al., 1993; Waychunas et al., 1993, 1996; Richmond et al., 2004). Thus, at an As/Fe molar ratio of 0.7 during precipitation, ferrihydrite units consisted mainly of Fe oxyhydroxyl octahedra arranged in short dioctahedral chains with minimal interchain linking by octahedral corners (Waychunas et al., 1993, 1996). In this study it was found that co-precipitation of trace amounts of arsenate with ferrihydrite with As/Fe molar ratio less than 0.005 induced no systematic change in the surface area or the structural disorder of ferrihydrite with increasing arsenate concentration (Pedersen et al., 2006).

The presence of trace amounts of arsenate during the oxidation of  $\text{Fe}^{2+}$  to either lepidocrocite or goethite, resulted in the adsorption of all the arsenate to the surface of lepidocrocite, whereas only 30% of the arsenate adsorbed on the surface of goethite while the remainder was bound so strongly that it did not desorb easily (Pedersen et al., 2006). Studies with schwertmannite, a poorly crystalline iron oxyhydroxysulfate whose structure includes tunnels that are stabilized by the presence of sulphate, have shown that arsenate is mainly adsorbed to the outside of the crystal and does not substitute for sulphate in the tunnels (Waychunas et al., 1995b). As in the case with ferrihydrite, the presence of arsenate during synthesis disrupt the structure of schwertmannite and at higher arsenate concentrations an amorphous Fe-arsenate phase is formed (Waychunas et al., 1995b; Carlson et al., 2002; Regenspurg et al., 2002; Regenspurg and Peiffer, 2005).





## 4 Reductive dissolution of iron oxides

Fe(III) oxides can be dissolved in two chemically different pathways; non-reductive or reductive. The non-reductive dissolution is promoted by either protons or ligands, such as oxalate or citrate, and occurs directly without change in the oxidation state and thus  $\text{Fe}^{3+}$  is released. Reductive dissolution is more complex than non-reductive dissolution because it involves an electron transfer from the reductants to the Fe(III), reducing it to Fe(II) which may subsequently accumulate in solution. The mechanism controlling the dissolution process depends on the presence and reactivity toward the surface of protons, ligands and reductants (Afonso et al., 1990). However, in natural waters, reductive dissolution is the predominating mechanism dissolving the iron oxides. In freshwater environments reductive dissolution is most often microbially mediated (Lovley, 1997) whereas in marine sediments abiotic reduction of iron oxides by  $\text{H}_2\text{S}$  is also of importance (Poulton, 2003).

### 4.1 Abiotic reductive dissolution

The theory for abiotic reductive dissolution of iron oxides is well established and is based on the surface complexation model. According to this model the surface of iron oxides contains hydroxyl surface groups with well defined coordinative properties for the interaction with the dissolution promoting species such as  $\text{H}^+$ ,  $\text{OH}^-$ , metal ions, anions, weak acids and other ligands (Zinder et al., 1986; Hering and Stumm, 1990; Stumm, 1992). The first step in the dissolution sequence is the adsorption of the reductant to the iron oxide surface and the formation of a surface complex. Thereafter an electron is transferred from the reductant to the Fe(III) oxide within this surface complex, resulting in an oxidized reactant. The electron may move freely in the surface layer of the oxide until it is consumed by the Fe(III) atom that becomes the centre of the detachable group, thereby producing Fe(II) on the surface (Zinder et al., 1986). The Fe(II)-oxygen bond in the surface of the crystalline lattice is more labile than the Fe(III)-oxygen bond and the reduced metal centre is therefore more easily detached from the surface than the original oxidized metal centre. The detachment of Fe(II) is considered as the slowest of the steps and therefore rate limiting. The detachment is accelerated by protonation of surface sites adjacent to the Fe(II) leaving the surface of the crystal (Hering and Stumm, 1990; Suter et al., 1991; Stumm, 1992).

Reductive dissolution of iron oxides can be accomplished with many reductants, such as ascorbic acid, phenols, dithionite,  $\text{HS}^-$  (Stumm, 1992). Those reductants, such as ascorbic acid, that form inner-sphere surface complexes are especially efficient (Stumm, 1992). In principle, all organic matter is thermodynamically apt to reduce Fe(III), and due to the high affinity of carboxylate groups for Fe(III) in solution or on the surface of a hydrous Fe(III) oxide, this type of process is very likely to occur in natural water, soils, and sediments. Furthermore, in marine environments, high in sulphate, reduction of iron oxides by sulphide produced by sulphate reduction is important.

Rates of reductive dissolution are significantly enhanced by the presence of ligands as shown by the combination dithionite/citrate (Mehra and Jackson, 1958)

and ascorbate/oxalate (Zinder et al., 1986; Banwart et al., 1989). The accelerating effect of the ligands is attributed to facilitation of the detachment of the reduced iron centre from the crystal lattice (Hering and Stumm, 1990).

The initial rate of hematite dissolution at pH 3 by the various dissolution mechanisms was investigated by Banwart et al. (1989). The dissolution rate increased in the order proton-assisted dissolution < ligand-promoted dissolution (50  $\mu$ M oxalate) < reductive dissolution (10 - 500  $\mu$ M ascorbate) < ligand-promoted reductive dissolution (100  $\mu$ M ascorbate + 50  $\mu$ M oxalate) with a factor of 350 between the extremes. A similar factor (400) has been found for goethite (Zinder et al., 1986).

#### 4.1.1 $\text{Fe}^{2+}$ catalysed dissolution of Fe(III) oxides

In the presence of a suitable ligand, the dissolution of both ferrihydrite (Fischer, 1972), goethite (Fischer, 1972; Hering and Stumm, 1990; Suter et al., 1991; Ballesteros et al., 1998), hematite (Hering and Stumm, 1990; Sulzberger et al., 1989) and magnetite (Hering and Stumm, 1990) is significantly accelerated by the presence of Fe(II).  $\text{Fe}^{2+}$  acts as a catalyst and there is no net reduction. The concentration of  $\text{Fe}^{2+}$  remains constant, while the concentration of  $\text{Fe}^{3+}$  increases.

The mechanism is believed to be an electron transfer from Fe(II) through the ligand to Fe(III) in the crystal lattice (Fischer, 1972; Sulzberger et al., 1989; Hering and Stumm, 1990; Suter et al., 1991; Stumm, 1992). Suitable ligands for the  $\text{Fe}^{2+}$  catalysed dissolution of iron oxides include oxalate, malonate, citrate, NTA and EDTA (Fischer, 1972; Sulzberger et al., 1989; Hering and Stumm, 1990; Suter et al., 1991; Ballesteros et al., 1998). In contrast Wehrli et al. (1989) and Suter et al. (1991) argued that  $\text{OH}^-$  is not a suitable ligand due to the insolubility of the Fe(III) hydroxo complex which enhances the chance of a reverse electron transfer and desorption of  $\text{Fe}^{2+}$ .

The requirement of a ligand to facilitate the dissolution of iron oxides by catalysed  $\text{Fe}^{2+}$  has been attributed to an increased adsorption of  $\text{Fe}^{2+}$  in the presence of a ligand and to facilitation of the detachment of Fe(III) from the surface (Wehrli et al., 1989). It has also been hypothesised that the electron transfer does not occur in the absence of a suitable ligand, and that the ligand acts as an electron bridge (Suter et al., 1991; Stumm, 1992). For an electron transfer to occur, the Fe(III) and the  $\text{Fe}^{2+}$  have to encounter each other in a suitable structural arrangement. In the case of Fe(II) acting as a reductant through a ligand, a ternary surface complex is formed and an electron transfer, presumably inner-sphere, occurs between the adsorbed Fe(II) and the surface Fe(III) followed by the rate-limiting detachment of the reduced surface iron (Hering and Stumm, 1990).

## 4.2 Biotic reduction

In natural sediments the reduction of iron oxides can function as the terminal electron accepting step in the process of organic matter degradation and is often catalysed by Fe(III) reducing micro-organisms (Lovley, 1997). Microbial Fe(III) reduction is commonly referred to as dissimilatory iron reduction and in this process the micro-organisms transfer electrons to external Fe(III), reducing it to Fe(II) for a purpose other than assimilation of iron into the biomass (Lovley, 2000). Known dissimilatory

Fe(III) reducing micro-organisms fall in a number of different phylogenetic groups suggesting that the ability to reduce Fe(III) is spread throughout the domain *Bacteria* (Lonergan et al., 1996). Fe-reducing organisms have been isolated from diverse environments including limnic and marine surface sediments, soils and aquifer sediments (Thamdrup, 2000), however, relative little is known of which organisms are most important in different sedimentary environments (Luu and Ramsay, 2003). The two most intensely studied genera of Fe(III) reducers are *Geobacter* and *Shewanella* which are often isolated from sedimentary environments, including the subsurface (Lovley, 1997).

Although poorly crystalline iron oxides generally constitutes approximately 20% or less of the Fe(III) in a sediment, they are the primary source of microbial Fe(III) oxide reduction (Thamdrup, 2000; Luu and Ramsay, 2003). Studies with the bacterium *Geobacter metallireducens* show that reduction of the crystalline iron oxides akaganeite, goethite, hematite and magnetite is very slow and that growth only occurs with ferrihydrite (Lovley and Phillips, 1988). Reduction rates decreased with increasing thermodynamic stability of the oxides in analogy to the observations with chemical reduction of Fe(III) oxides (Larsen and Postma, 2001).

While the rate limiting step in abiotic reductive dissolution of iron oxides is generally considered to be the detachment of Fe(II) from the crystal lattice (Zinder et al., 1986), the rate limiting step is still unclear for biotic reduction of iron oxide. Several observations have lead to the hypothesis that the reduction mechanism of biologically mediated iron oxide reduction is fundamentally different from that of abiotic reductive dissolution (Roden, 2003a,b). One reason is that while the oxide surface area appears to exert primary control on initial rates of bacterial reduction with oxide crystal thermodynamic properties (e.g.  $\Delta G_f$ ,  $K_{sp}$ ) playing a comparatively minor role (Roden and Zachara, 1996; Roden, 2003b), the effect of the iron oxide mineralogy on the abiotic reduction is strong while, for the different iron oxides, the abiotic initial rate was independent of the specific surface area (Larsen and Postma, 2001). A recent study showed, however, a strong correlation between microbial reduction rate and the solubility of iron oxides indicating that the reductive activity of the cells is a function of the mineral lattice in which the Fe(III) surface centre is embedded (Bonneville et al., 2004). Furthermore, initial rate with ascorbate as reductant vary by more than 3 orders of magnitude depending on the oxide mineralogy, in comparison to the ca. one order of magnitude variation in rates of enzymatic, biotic, reduction regardless of the fact that apart from different iron oxides also different organisms, substrate etc. are employed (Roden, 2003a,b).

Considering the tendency for Fe(II) to reassociate (or never become detached in the first place) with oxide surfaces during enzymatic reduction at circumneutral pH, the kinetics of bacterial iron reduction may not be controlled by the release of Fe(II). Instead the rate of electron transfer (Roden, 2003b) and the adsorption of Fe(II) to either the oxide or the cell surface (Roden, 2003a), thereby protecting the Fe(III) oxide, has been proposed as the rate limiting step in enzymatic iron oxide reduction.

### 4.2.1 Mechanisms of bacterial electron transfer

For micro-organisms utilizing soluble inorganic substrates like oxygen, nitrate and sulphate, the soluble nutrients and substrate enter the bacterial cell through the cell wall. However, the dominating form of Fe at neutral pH is solid phase Fe and therefore Fe(III) cannot diffuse through the cell wall and into the cell. The mechanism of microbial electron transport to insoluble acceptors is poorly understood and a major question is therefore how the Fe(III) reducers access the Fe(III) oxides. Until recently, it was generally considered that Fe(III)-reducing micro-organisms reduced these Fe(III) oxides by establishing direct contact with the Fe(III) oxide in order to transfer electrons from the cell to the Fe(III) oxide surface (Lovley and Phillips, 1988; Kostka and Nealson, 1995; Roden and Zachara, 1996; Das and Caccavo, 2000; Thamdrup, 2000). However, a number of potential alternative strategies are now recognized in which Fe(III)-reducing micro-organisms do not need to be in direct contact with the Fe(III) oxides.

One alternative strategy is solubilisation of the solid phase iron by high-affinity Fe(III) chelators, the so-called siderophores. The siderophores are water-soluble, low molecular weight, Fe(III)-specific ligands which are induced at low iron concentrations (Luu and Ramsay, 2003) to facilitate solubilisation of Fe(III) making it more accessible to the micro-organisms and enabling transport into or close to the cell (Madigan et al., 2003).

Electron-shuttling compounds may provide another mechanism of alleviating the need for Fe(III)-reducing micro-organisms to directly contact Fe(III) oxides in order to reduce them. An effective electron shuttle can accept electrons from Fe(III)-reducing micro-organisms and then transfer the electrons to the Fe(III) oxide surface, regenerating the electron shuttle in the oxidized form. In this manner, small amounts of an electron shuttle can act as catalyst and undergo multiple reduction-oxidation cycles (Nevin and Lovley, 2002b). The first electron shuttling compounds reported to stimulate iron oxide reduction were humic substances and related compounds (Lovley et al., 1996). Humic substances have been suggested as being the most common alternative electron acceptor for Fe-reducing bacteria (Lovley et al., 1996; Lovley, 1997; Thamdrup, 2000; Straub et al., 2001; Nevin and Lovley, 2002a,b). It has also been proposed that Fe(III)-reducing micro-organisms might synthesize and release electron shuttling compounds (Nevin and Lovley, 2002b; Seeliger et al., 1998; Nevin and Lovley, 2000; Turick et al., 2002; Newman and Kolter, 2000).

Most recently, it has been proposed that some micro-organisms may transfer electrons from the cell surface to the surface of Fe(III) oxides through biological nanowires (Reguera et al., 2005).

## 4.3 Reactivity

### 4.3.1 Rate expression

The kinetics of iron oxide dissolution have been extensively studied using various reactants and/or different iron oxide minerals, and several rate equations for iron oxide dissolution exists (Cornell and Schwertmann, 2003). Postma (1993) applied the general rate law for mineral dissolution (Christoffersen and Christoffersen, 1976) to

determine the reactivity of iron oxides:

$$J = \frac{d\left(\frac{m}{m_0}\right)}{dt} = k \cdot m_0 \cdot f\left(\frac{m}{m_0}\right) \cdot g(C) \quad (4.1)$$

In this rate law,  $J$  is the overall rate of dissolution (mol/s),  $m_0$  is the initial mass of crystal,  $m$  is the mass of crystals at time  $t$ , and  $k$  is the rate constant ( $\text{s}^{-1}$ ). The term  $f(m/m_0)$  is a function of the undissolved crystal fraction usually described by  $(m/m_0)^\gamma$  and accounts for changes in mineral crystal size, morphology, reactive site density, etc., whereas  $g(C)$  is a function of the solution composition e.g. the type and concentrations of the reactant and pH. Hence, the effects of the crystals and of the solution composition is separated in Eqn. 4.1 and may consequently be investigated under different experimental conditions. The effect of the reactant on iron oxide dissolution is investigated if  $f(m/m_0)$  is kept constant in the course of the experiment as is the case in initial rate dissolution experiments where only a negligible fraction of the iron oxide dissolves. If, on the other hand, the reactivity of the iron oxides is studied,  $g(C)$  should be kept constant. By using a high concentration of the reactant and only a small amount of iron oxide, the solution composition changes only marginally and  $g(C)$  can be assumed to be constant. In case of constant  $g(C)$ , Eqn. 4.1 is reduced to

$$\frac{J}{m_0} = k' \cdot \left(\frac{m}{m_0}\right)^\gamma \quad (4.2)$$

where  $k'$  ( $\text{s}^{-1}$ ) contains both the rate constant and  $g(C)$  while  $\gamma$  expresses the change in the dissolution rate during dissolution. Approximating the particles by uniform spheres or cubes, gives a theoretic value of  $\gamma$  of  $2/3$  based on the relation between surface area and crystal mass (Christoffersen and Christoffersen, 1976; Larsen and Postma, 2001). However, experimental  $\gamma$ -values are often higher than the theoretical value indicating the importance of other factors such as changes in surface area, grain size distribution, differences in the reactivity of different crystal planes and reactive site density etc. during the dissolution (Larsen and Postma, 2001).

### 4.3.2 Reactivity of iron oxides

Postma (1993) developed a method by which the reactivity of iron oxides is determined by reductive dissolution of the iron oxides in 10 mM ascorbic acid at pH 3 and subsequent fitting of the data to Eqn. 4.2. A comparison of the reactivity of ferrihydrite, lepidocrocite, goethite and hematite obtained by Larsen and Postma (2001) and in this study (Pedersen et al., 2005, 2006) is shown in Figure 6 showing  $\log(J/m_0)$  versus  $\log(m/m_0)$ . Displayed like this, the rate expression 4.2 gives a straight line with a slope equal to  $\gamma$  and an interception with the  $\log(J/m_0)$ -axis equal to  $k'$ .

Figure 6 displays ferrihydrite and lepidocrocite as the most reactive iron oxides with initial reduction rate ( $k'$ ) in the range  $4 - 7 \cdot 10^{-4} \text{ s}^{-1}$  and  $3 \cdot 10^{-5} - 1 \cdot 10^{-4} \text{ s}^{-1}$ , respectively, while goethite and hematite are less reactive with  $k'$  in the order of  $10^{-6}$  and  $10^{-7} \text{ s}^{-1}$ , respectively (Postma, 1993; Larsen and Postma, 2001; Pedersen et al., 2005, 2006). Lepidocrocite shows some variation in the reactivity which covers variations in synthesis conditions such as temperature, Cl/Fe ratio and pH (Postma, 1993; Pedersen et al., 2005). But still, given the different synthesis and repeated synthesis of the iron oxides, the oxides show a quite remarkable small range in the variation of reduction rates.

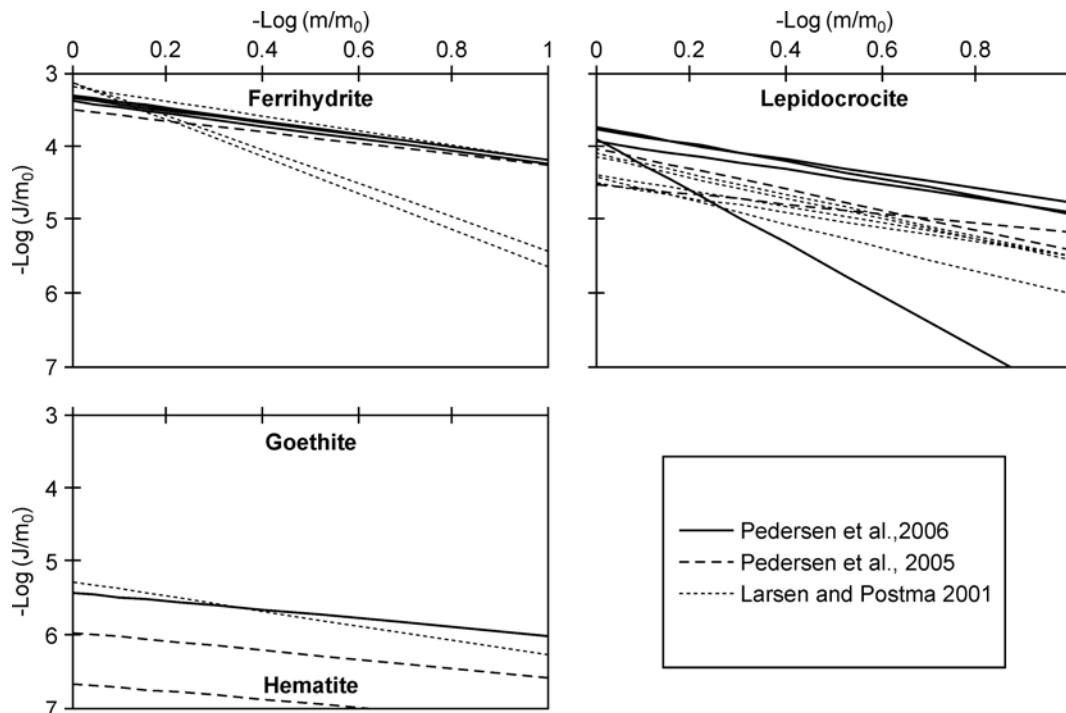


Figure 6: Comparison of iron oxide reactivity displayed as reduction rates normalized over initial mass ( $J/m_0$ ) versus the fraction of remaining oxide ( $m/m_0$ ) for ferrihydrite, lepidocrocite, goethite and hematite.

The initial rate, normalized to surface area, is displayed against the specific surface area in Figure 7 and these two parameters show no simple correlation in this extended data set in accordance with the findings of Larsen and Postma (2001). In contrast, the linear correlation between the initial specific reduction rate of lepidocrocite and surface area as found by (Larsen and Postma, 2001) seems more questionable in Figure 7 as the correlation coefficient,  $r^2$  is 0.49. This shows the importance of other factor than the surface area on the reductive dissolution rate. Especially, the temperature for the synthesis seems to have an impact on the dissolution rate which may be due to a strong correlation between the temperature for the synthesis and the surface area. Another factor that may be of importance is the oxidation rate, however, it was not possible to quantify the importance of the oxidation rate on the reductive dissolution rate.

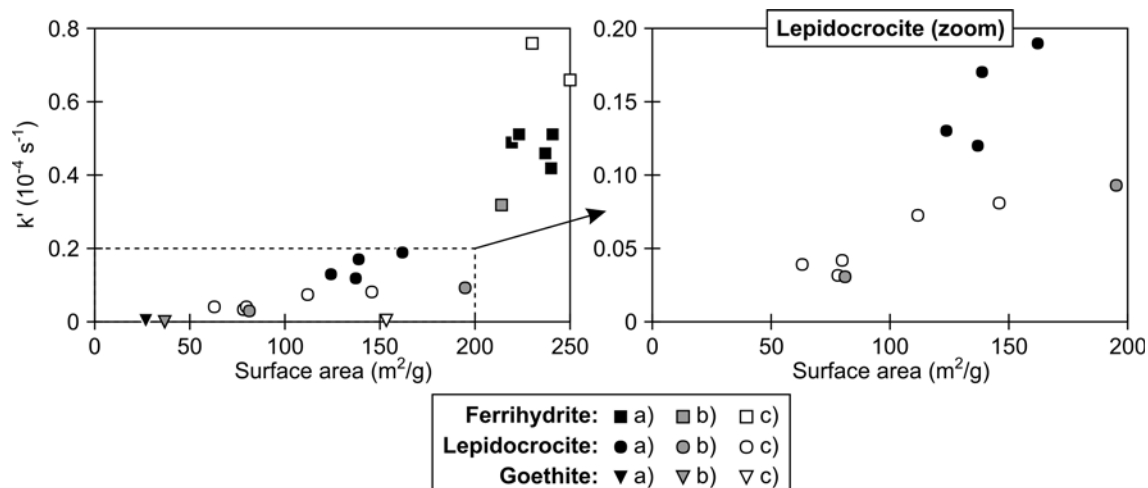


Figure 7: Initial reduction rates of ferrihydrite, lepidocrocite and goethite as a function of specific surface area as found by a) Pedersen et al. (2006), b) Pedersen et al. (2005) and c) Larsen and Postma (2001). The figure to the right shows the dependence of the initial reduction rate of lepidocrocite on the surface area.

#### 4.3.3 Effect of arsenate on the reactivity of the iron oxides

Since dissolution of iron oxides is a surface controlled reaction, it may be inhibited or enhanced by substances adsorbed to the surface (Hering and Stumm, 1990; Stumm, 1992; Biber et al., 1994). The effect of oxyanions on the dissolution of iron oxides has been studied under varying conditions such as the type of iron oxide, the dissolution pathway, the oxyanion/Fe molar ratio and pH (Bondietti et al., 1993; Biber et al., 1994; Paige et al., 1997a; Eick et al., 1999). Both an inhibitory (Bondietti et al., 1993; Biber et al., 1994; Paige et al., 1997a; Eick et al., 1999) and an accelerating effect (Bondietti et al., 1993; Eick et al., 1999) have been observed but which conditions favour one effect over the other remains unclear. For example, Bondietti et al. (1993) observed that arsenate inhibits the dissolution of lepidocrocite by EDTA at pH 7, but accelerated the dissolution at pH 3. In contrast, Eick et al. (1999) found an acceleration of oxalate promoted dissolution of goethite at pH 6, but an inhibition at lower pH. The inhibitory effect of oxyanions on the dissolution of iron oxides has been ascribed to the adsorption of binuclear surface complexes (Bondietti et al., 1993; Biber et al., 1994; Stumm, 1995; Paige et al., 1997a; Eick et al., 1999) whereas the accelerating effect has been attributed to the formation of mononuclear surface complexes (Bondietti et al., 1993) and increased proton adsorption due to increased negative surface charge owing to adsorption of arsenate (Eick et al., 1999). Inhibition by arsenate of the microbial mediated dissolution of schwertmannite at pH 2 was ascribed to reduced solubility of schwertmannite, thereby reducing the pool of soluble Fe(III) utilized by the reducing bacterium (Regenspurg et al., 2002).

In this study arsenate was coprecipitated with ferrihydrite, lepidocrocite and goethite in the As/Fe molar ratio 0 - 0.005, 0 - 0.005, and 0 - 0.001, and no systematic correlation between the arsenate content and the reactivity of the iron oxides



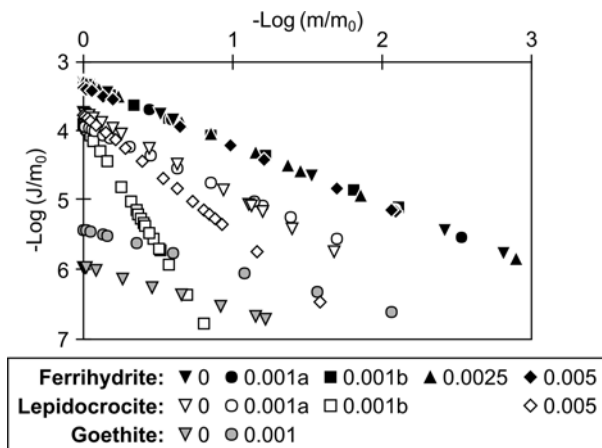


Figure 8: Comparison of the reduction rates, normalized over initial mass ( $J/m_0$ ) versus the fraction remaining in the solid phase ( $m/m_0$ ) for ferrihydrite, lepidocrocite and goethite with various As/Fe molar ratios. The legend denotes the molar ratio of the iron oxides.

was found (Fig. 8). Even though Biber et al. (1994) found a significant inhibitory effect of phosphorus on the reductive dissolution of hematite by  $H_2S$  at a phosphorus concentration as low as  $10 \mu M$ , the potential effect of an adsorbed anion on the dissolution rate must depend on the fraction of surface sites occupied by the anion, since dissolution of iron oxides is a surface controlled process. As a best approximation of the As/surface site ratio, the As/Fe ratio is used to compare the results of in this study with previous studies. Since previous studies (Bondietti et al., 1993; Biber et al., 1994; Paige et al., 1997a; Eick et al., 1999) generally have used significantly higher As/Fe molar ratios (0.002 - 5.6), the insensibility of the reduction rate towards trace amounts of arsenate is attributed to the low arsenate concentration employed here. Furthermore, in contrast to adsorption experiments, an additional variability is added to the reduction rate in coprecipitation experiments, due to the natural variation between separately synthesized oxides (Fig. 6), and a potential effect of trace amounts of arsenic may not be visible compared to the variation between the iron oxides.

#### 4.4 Release of arsenate during reduction of iron oxides

The release of arsenate during proton assisted dissolution of ferrihydrite in a  $HNO_3$  solution with pH 1.3 was studied by Paige et al. (1997a) who observed an incongruent release of arsenate and Fe(III) upon dissolution of the oxide. In this study radioactive  $^{73}As$  was used to investigate the release of arsenate during reductive dissolution of iron oxides in 10 mM ascorbic acid at pH 3. The application of radio labelled arsenate enables precise measurement of even small concentrations of arsenate since all isotopes of an element are expected to behave identically, except for very minor mass effects, and release of the bulk of arsenate therefore follows that of  $^{73}As$ . The iron oxides employed in this study were ferrihydrite, lepidocrocite and goethite coprecipitated in the presence of arsenate at an As/Fe molar ratio of 0.001

to 0.005, 0.001 to 0.005 and 0.001, respectively. The arsenate was not reduced to arsenite during the reductive dissolution of the iron oxides.

The release of arsenate during the reductive dissolution of ferrihydrite, lepidocrocite and goethite is compared to the release of  $\text{Fe}^{2+}$  in Figure 9 showing the fraction of  $^{73}\text{As}$  released as a function of the fraction of  $\text{Fe}^{2+}$  over total Fe released. The straight line represents congruent release of arsenate and  $\text{Fe}^{2+}$  during the reductive dissolution of the iron oxide. Points that plot along the line with a smaller slope indicate a slower release of arsenate compared to  $\text{Fe}^{2+}$  whereas points following a larger slope indicate that relative more arsenate is present in solution compared to  $\text{Fe}^{2+}$ .

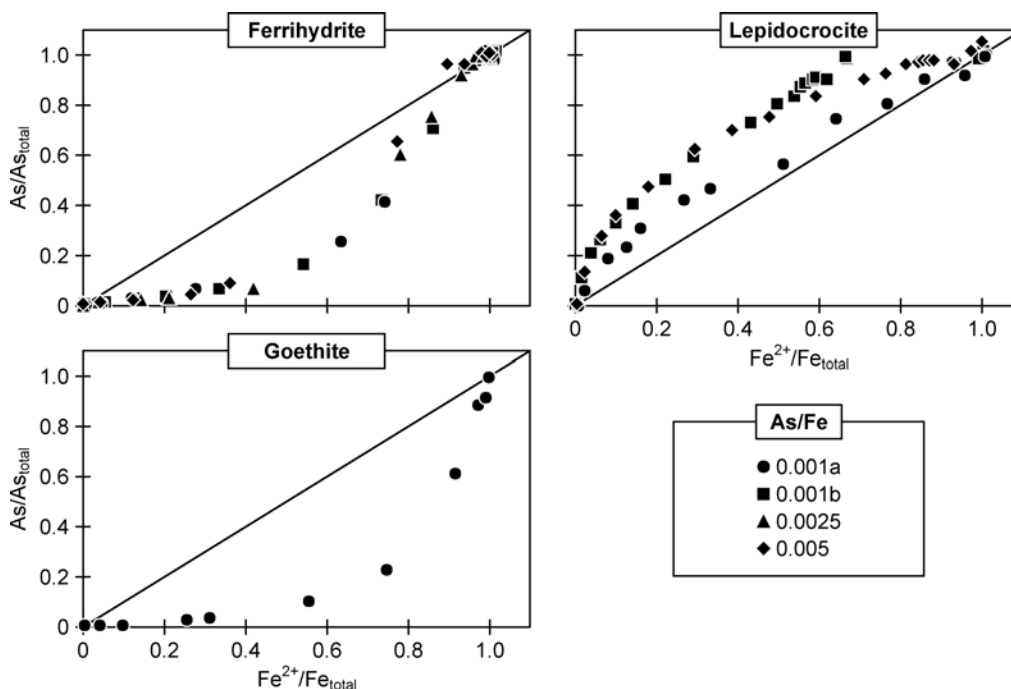


Figure 9: Relative release of  $^{73}\text{As}$  versus the relative release of  $\text{Fe}^{2+}$  during reductive dissolution of ferrihydrite, lepidocrocite and goethite at various As/Fe ratios.

Figure 9 depicts a highly incongruent release of arsenate from ferrihydrite, lepidocrocite and goethite during reductive dissolution of the iron oxides. However, the behaviour of arsenate differs with the iron oxide. While the release of arsenate is significantly retarded compared to the release of  $\text{Fe}^{2+}$  during the reductive dissolution of ferrihydrite and goethite, arsenate is preferentially desorbed from lepidocrocite. In this study a method was developed, by which the adsorbed arsenate was determined by extracting the  $^{73}\text{As}$  adsorbed to the iron oxide in a  $250\ \mu\text{M}$  arsenate solution. This enables the determination of adsorbed arsenate during the reductive dissolution of the iron oxides (Fig. 10). Nearly all the arsenate was extracted by this method during reductive dissolution of ferrihydrite and lepidocrocite indicating that the arsenate was not incorporated into the structure of either iron oxide. In contrast, only approximately 30% of the arsenate was extracted at the beginning

of the dissolution experiment with goethite, showing that a large fraction of the arsenate is firmly bound within the structure of goethite.

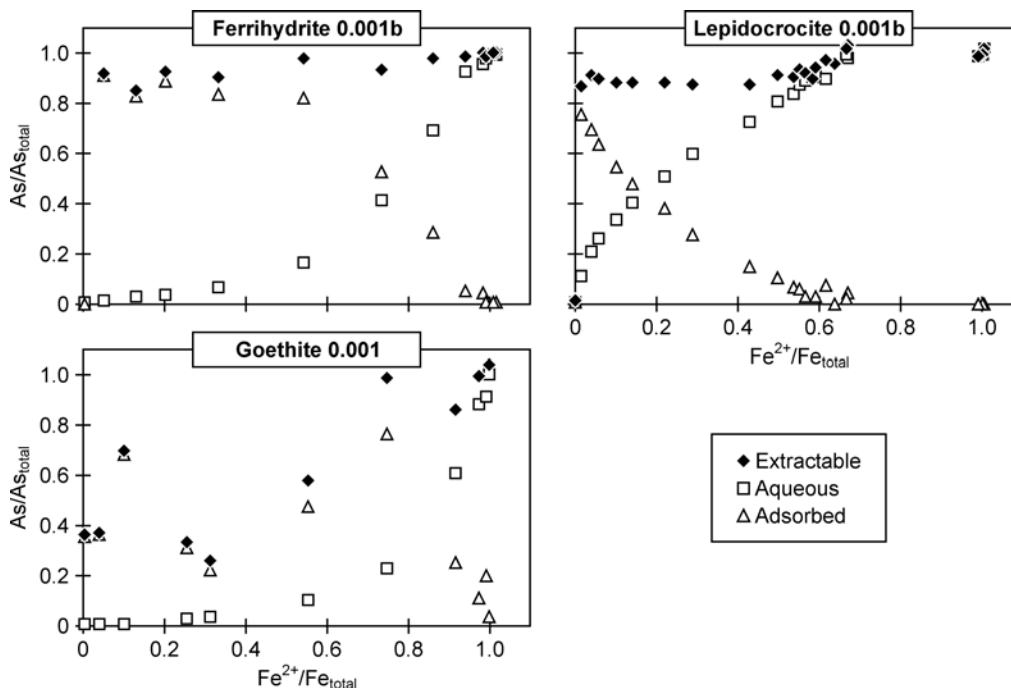


Figure 10: The fraction of adsorbed and aqueous arsenate ( $^{73}\text{As}/^{73}\text{As}_{\text{total}}$ ) versus the fraction of dissolved crystal ( $\text{Fe}^{2+}/\text{Fe}^{2+}_{\text{total}}$ ) during reductive dissolution of Ferrihydrate 0.001b, Lepidocrocite 0.001b and Goethite 0.001. Extractable corresponds to the sum of adsorbed and aqueous arsenic

During reductive dissolution of ferrihydrite, arsenate remains adsorbed to the surface of the oxide until approximately 50% of the oxide has dissolved after which a decrease in the adsorbed arsenate is correlated with an increase in aqueous arsenate. A similar pattern is observed for goethite. The retarded release of arsenate from ferrihydrite and goethite was attributed to a strong adsorption of arsenate onto the surface of the iron oxide until saturation of the surface sites with arsenate is achieved after which arsenate is released as the iron oxide is further reduced (Pedersen et al., 2006). Using a sorption density of 2.6 sites/nm<sup>2</sup> for ferrihydrite (Dixit and Hering, 2003) and assuming all the arsenate was adsorbed, it was estimated that approximately 1% of the surface of ferrihydrite was covered with arsenate prior to dissolution, at all the investigated As/Fe molar ratios investigated. Hence, it seems reasonable that the surface of ferrihydrite is not saturated with arsenate until a significant part of the oxide has dissolved.

In contrast, adsorbed arsenate decreases initially during reductive dissolution of lepidocrocite (Fig. 10) causing a faster release of arsenate than  $\text{Fe}^{2+}$  during the reductive dissolution (Fig. 9). Since arsenate adsorbs to lepidocrocite through bidentate corner sharing between  $\text{AsO}_4$  tetrahedra and edge sharing pairs of  $\text{FeO}_6$  octahedra (<sup>2</sup>C in Fig. 5)(Randall et al., 2001), the possible sites for arsenate adsorption are along the b- and the c-axis, of which the c-axis is the primary sorbing face on lepidocrocite (Fig. 2). Larsen and Postma (2001) used Transmission Electron Mi-

crographs to conclude that lepidocrocite is reductively dissolved by ascorbate by etch-pitting of the crystals parallel to the c-axis, and apparently this eliminates the surface sites for adsorption of arsenate.

#### 4.4.1 PHREEQC simulation

The release of arsenate during reductive dissolution of ferrihydrite with an As/Fe molar ratio of 0.001 was modelled with the surface complexation model of Dzombak and Morel (1990) using the implementation in PHREEQC version 2.11.00 (Parkhurst and Appelo, 1999). An arsenate containing solution with pH 3 was equilibrated with ferrihydrite and the saturation index set to -5 to prevent an increase in aqueous  $\text{Fe}^{3+}$ . The adsorption of arsenate onto ferrihydrite was obtained by addition of a surface with the number of surface sites related to the amount of ferrihydrite. The reductive dissolution of ferrihydrite was modelled by addition of  $\text{H}_2$ . As oxidation of  $\text{H}_2$  is an acid producing reaction and reduction of iron oxides is an acid consuming process, the pH only increased slightly from pH 3 to 3.1 during the simulations.

Table 2: PHREEQC results

Model	$\log(K_1)$ <sup>a</sup>	$\log(K_2)$ <sup>b</sup>	$\log(K_3)$ <sup>c</sup>	Sites mol/mol Fe	Surface area $\text{m}^2/\text{mol}$
Dzombak and Morel (1990)	29.31	23.51	10.58	0.20	$5.33 \cdot 10^4$
Dixit and Hering (2003)	29.88	24.51	18.10	0.24	$5.33 \cdot 10^4$
Fit, Default surface area	29.31	26.70	10.58	0.0099	$5.33 \cdot 10^4$
Fit, Measured surface area	29.31	23.51	10.58	0.0065	$2.11 \cdot 10^4$ <sup>d</sup>

<sup>a</sup>Equilibrium constant for  $\text{Hfo\_wOH} + \text{AsO}_4^{3-} + 3\text{H}^+ = \text{Hfo\_wH}_2\text{AsO}_4 + \text{H}_2\text{O}$

<sup>b</sup>Equilibrium constant for  $\text{Hfo\_wOH} + \text{AsO}_4^{3-} + 2\text{H}^+ = \text{Hfo\_wHAsO}_4^- + \text{H}_2\text{O}$

<sup>c</sup>Equilibrium constant for  $\text{Hfo\_wOH} + \text{AsO}_4^{3-} = \text{Hfo\_wOHAsO}_4^{3-}$

<sup>d</sup>Determined by BET

In model 1, the standard setup in the Dzombak and Morel (1990) database was used (Table 2), and in model 2 the complexation constants of arsenate sorption on ferrihydrite and the sorption density obtained by Dixit and Hering (2003) was applied. The two models give nearly the same result and neither of the models agree well with the measured data (Fig. 11). Both models predict arsenate to be adsorbed much stronger to the oxide surface than indicated by the measured data.

To get a conceptual understanding of which of the parameters are responsible for the difference, the intrinsic equilibrium constant for arsenate sorption and the site density in the Dzombak and Morel (1990) database were fitted to the measured data. Reasonable fits (Fig. 11) are obtained using the default surface area of  $600 \text{ m}^2/\text{g}$  and a site density of  $0.0099 \text{ mol/mol Fe}$ , or using the measured surface area and a site density of  $0.0065 \text{ mol/mol Fe}$ , and in both cases changing the second equilibrium constant from  $\log(K_2) = 23.51$  to  $\log(K_2) = 26.7$  (Table 2).

The significantly lower site density is attributed to competition for the sorption sites from ascorbic acid in the experiment, lowering the sites available for arsenate. At the  $10 \text{ mM}$  ascorbic acid applied in the reductive dissolution experiment, the

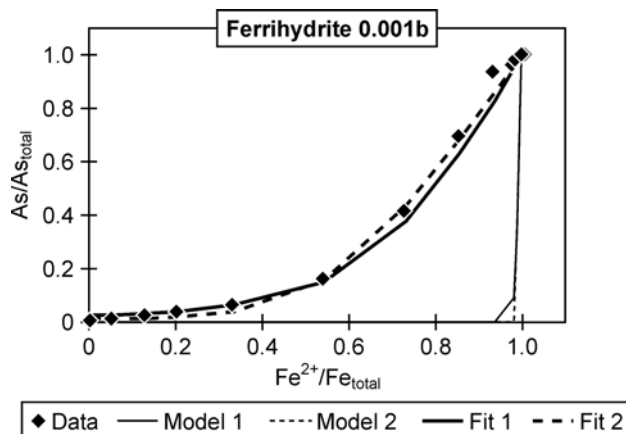


Figure 11: Comparison of the results of the PHREEQC simulations with the measured data. Detailed information about the models are found in Table 2.

surface of ferrihydrite is saturated with ascorbic acid to keep the reduction rate independent of the ascorbic acid concentration (Banwart et al., 1989; Postma, 1993). It is therefore not unreasonable to expect ascorbic acid to dominate at the ferrihydrite surface. Unfortunately, it has not been possible to include the presence of ascorbic acid in the model owing to a lack of surface complexation constants for ascorbic acid on iron oxides. A fit of the data for As/Fe ratios of 0.0025 and 0.005 results in an increase in the site density to 0.011 mole/mole Fe and 0.017 mole/mole Fe, respectively. This linear correlation ( $r^2 = 0.996$ ) between the arsenate content and the fitted site density is in line with a competitive equilibrium between the ascorbic acid and arsenate on the surface of ferrihydrite.

## 5 Transformation of iron oxides

### 5.1 General

A characteristic of the iron oxide system is the variety of possible interconversions between the different phases. Under appropriate conditions, almost every iron oxide can be converted into at least two other more stable phases. Structurally the transformations may proceed via two principally different mechanisms; either topotactic or reconstructive. Topotactic transformation occurs within the solid phase and therefore a correspondence in three dimensions between the initial and final structure is required. Usually, a topotactic transformation only takes place at elevated temperatures, as a certain mobility of the atoms is required.

A reconstructive transformation involves the dissolution of the initial phase and precipitation from solution of the new phase, and therefore no structural relationship is required between the precursor and the transformation product. Since the precursor dissolves, a reconstructive transformation depends on the solubility and dissolution rate of the precursor and may occur at ambient temperature.

The transformation of ferrihydrite and lepidocrocite to hematite is topotactic while the transformation of ferrihydrite to lepidocrocite and goethite and of lepidocrocite to goethite is reconstructive. The two processes are competitive, and conditions promoting goethite formation are therefore unfavourable for hematite formation and vice versa (Schwertmann and Murad, 1983).

The driving force for the transformations of iron oxides is the thermodynamic instability of the more unstable iron oxides such as ferrihydrite and lepidocrocite. Under oxic conditions, goethite and hematite are thermodynamically the most stable compounds and are therefore the end member of many transformation pathways (Cornell and Schwertmann, 2003). With decreasing redox potential, the iron oxides become thermodynamically unstable with respect to various ferrous containing solid phases of which magnetite, siderite and iron sulphides are the most stable (Zachara et al., 2002). Factors controlling the rate, the extent of transformation and the transformation product have been extensively studied in the laboratory (Cornell and Schwertmann, 2003), and include pH, foreign inorganic and organic ions, temperature and impurities of crystalline iron oxides.

The presence of foreign ions may affect the rate of transformation and/or the product into which ferrihydrite transforms. Most of the investigated species, including Al (Schwertmann et al., 2000), Si (Campbell et al., 2002) and P (Galvez et al., 1999), retard the transformation of ferrihydrite, suppress the formation of goethite and favours the formation of hematite in the transformation product. As the transformation rate is very low at room temperature, most studies have been conducted at elevated temperatures.

### 5.2 $\text{Fe}^{2+}$ catalysed transformation of Fe(III) oxides

The presence of  $\text{Fe}^{2+}$ , either added as Fe(II)-salts or produced by iron oxide reduction, catalyses the transformation of ferrihydrite and lepidocrocite to the more crystalline phases lepidocrocite and goethite (van Oosterhout, 1967; Fischer, 1972; Schwertmann and Taylor, 1973; Cornell and Schneider, 1989; Jang et al., 2003; Jeon

et al., 2003) or to the mixed valence Fe(II)-Fe(III) compound magnetite (Tamaura et al., 1983; Mann et al., 1989; Sørensen and Thorling, 1991; Jolivet et al., 1992). For example, the time of conversion of ferrihydrite to goethite at room temperature takes months in the absence of  $\text{Fe}^{2+}$  (Cornell and Schwertmann, 2003) but only days when  $\text{Fe}^{2+}$  is present (Jang et al., 2003; Pedersen et al., 2005). A high pH and a high Fe(II) to Fe(III) ratio seem to favour the formation of magnetite (Mann et al., 1989; Jolivet et al., 1992; Pedersen et al., 2005). Tronc et al. (1992) and Jolivet et al. (1992) examined the transformation of ferrihydrite at pH 8 and room temperature at varying Fe(II)/Fe(III) ratios and found that at a low  $\text{Fe}^{2+}$  concentration ferrihydrite was transformed into goethite whereas at a higher  $\text{Fe}^{2+}$  concentration magnetite was formed.

Only a few studies have examined the effect of  $\text{Fe}^{2+}$  on the transformation of goethite and hematite. During microbially mediated reduction of the iron oxides at pH 6-8, goethite and hematite remained unchanged at conditions where ferrihydrite transformed into magnetite (Zachara et al., 2002). Jeon et al. (2001) found a transformation of hematite to magnetite at pH higher than 6, whereas no transformation occurred at pH less than 6.

Table 3: Characteristics of the iron oxides used in this study

Iron oxide	Crystal size (nm)	Surface area ( $\text{m}^2/\text{g}$ )	Reactivity	
			$k'$ ( $\text{s}^{-1}$ )	$\gamma$
Ferrihydrite	–	214	$3.2 \cdot 10^{-4}$	0.75
Lepidocrocite #1	5	195	$9.3 \cdot 10^{-5}$	1.37
Lepidocrocite #2	20	81	$3.1 \cdot 10^{-5}$	0.66
Goethite	20	37	$1.1 \cdot 10^{-6}$	0.62
Hematite	40	19	$2.2 \cdot 10^{-7}$	0.54

In this study, the  $\text{Fe}^{2+}$  catalysed transformation of ferrihydrite, lepidocrocite, goethite and hematite at  $25^\circ\text{C}$  was studied using  $^{55}\text{Fe}$  labelled iron oxides. Two different lepidocrocites were employed; one synthesized at  $10^\circ\text{C}$  (Lepidocrocite #1) and another synthesized at  $25^\circ\text{C}$  (Lepidocrocite #2) resulting in a different surface area and reactivity (Table 3). The transformation of the iron oxides was investigated by submerging the oxides (0.5 mM) in solutions containing 0 to 1.0 mM  $\text{Fe}^{2+}$ , buffered to pH 6.5 with  $\text{HCO}_3^-$ . The solid phase was characterized by powder X-ray diffraction before and after the transformation (Pedersen et al., 2005).

Within two days, ferrihydrite transformed completely (within the detection limit of XRD) into lepidocrocite and goethite at an  $\text{Fe}^{2+}$  concentration of 0.2 and into goethite at an  $\text{Fe}^{2+}$  concentration of 1.0 mM. Lepidocrocite remained unchanged at 0.2 mM  $\text{Fe}^{2+}$  but was transformed into magnetite at the higher  $\text{Fe}^{2+}$  concentration, whereas no transformation to other phases was observed for goethite and hematite, even after 16 and 26 days, respectively. No transformation of any of the oxides was observed in the absence of  $\text{Fe}^{2+}$ .

To follow the transformation of the iron oxides trace amounts of  $^{55}\text{Fe}$  were incorporated in the structure of the iron oxides. The applicability of  $^{55}\text{Fe}$  as a tracer was tested by monitoring the release of  $\text{Fe}^{2+}$  and  $^{55}\text{Fe}$  during reductive dissolution of the radio labelled iron oxides in 10 mM ascorbic acid at pH 3. The  $^{55}\text{Fe}$  was released

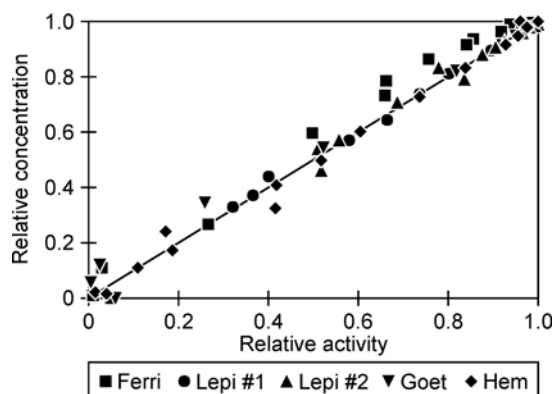


Figure 12: The release of  $\text{Fe}^{2+}$  versus the release of  $^{55}\text{Fe}$  during reductive dissolution of ferrihydrite (Ferri), lepidocrocite synthesized at  $10^\circ\text{C}$  (Lepi #1) and at  $25^\circ\text{C}$  (Lepi #2), goethite (Goet) and hematite (Hem) in 10 mM ascorbic acid at pH 3. Concentrations and activities are normalized to the added amount. The line represents congruent release. With permission from Elsevier.

congruently ( $r^2 = 0.977$  to  $0.989$ ) with  $\text{Fe}^{2+}$  during the reductive dissolution (Fig. 12) indicating a homogeneous distribution of the tracer within the iron oxides.

The activity of aqueous  $^{55}\text{Fe}^{2+}$  in the transformation experiments with  $^{55}\text{Fe}$ -labelled ferrihydrite suspended in solutions with variable  $\text{Fe}^{2+}$  concentrations is shown in Figure 13. In the absence of  $\text{Fe}^{2+}$ , where no transformation occurred, there is no release of  $^{55}\text{Fe}$ . In contrast, a significant and rapid increase in the activity of  $^{55}\text{Fe}$  is observed in the presence of  $\text{Fe}^{2+}$  as a result of the reaction between the iron oxides and  $\text{Fe}^{2+}$ . Within 24 hours, the release of  $^{55}\text{Fe}$  from ferrihydrite levels off and becomes constant at levels depending on the  $\text{Fe}^{2+}$ -concentration. The higher the  $\text{Fe}^{2+}$ -concentration, the higher the maximum  $^{55}\text{Fe}$ -activity released from ferrihydrite.

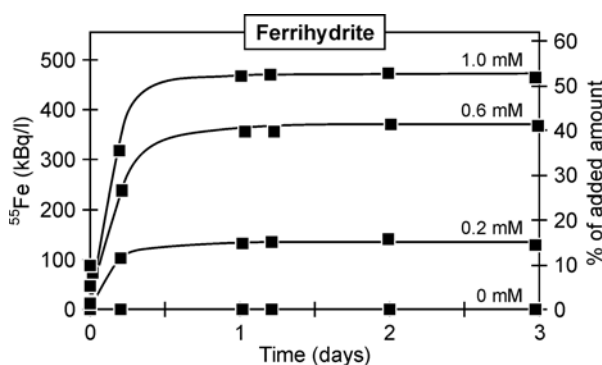


Figure 13: The release of  $^{55}\text{Fe}$  into solution in experiments with  $^{55}\text{Fe}$  labelled ferrihydrite dispersed in solutions containing 0, 0.2, 0.6 and 1.0 mM  $\text{Fe}^{2+}$ . Lines are provided for visual aid. With permission from Elsevier.



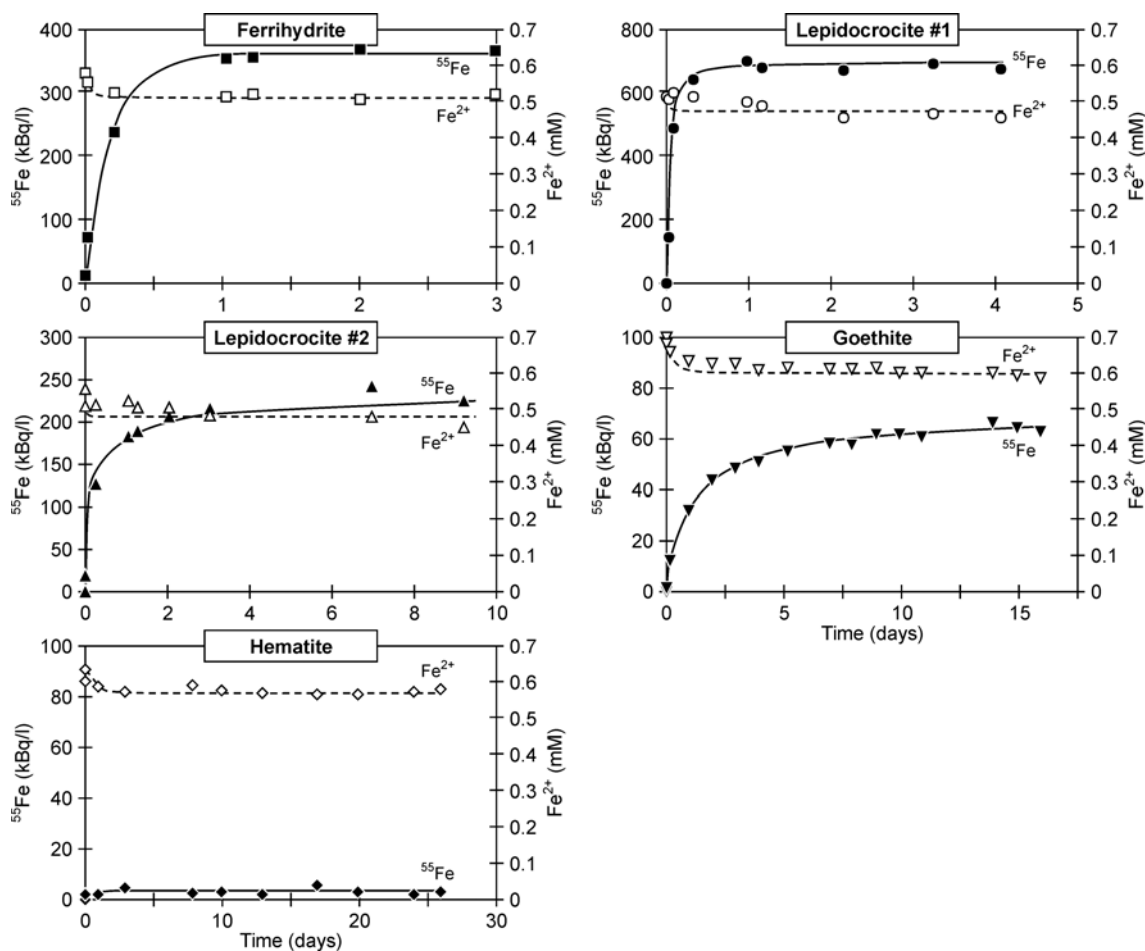


Figure 14: Aqueous  $\text{Fe}^{2+}$  concentration (open symbols) and release of  $^{55}\text{Fe}$  (filled symbols) from ferrihydrite, lepidocrocite #1 and #2, goethite and hematite. Initially the solutions contained 0.6 mM  $\text{Fe}^{2+}$ . Lines are provided for visual aid. With permission from Elsevier.

Although lepidocrocite and goethite did not transform during the experiments, they did react with  $\text{Fe}^{2+}$  as evidenced by the release of  $^{55}\text{Fe}$  from the oxides when  $\text{Fe}^{2+}$  is present (Fig. 14). However, while the release of  $^{55}\text{Fe}$  from ferrihydrite and lepidocrocite #1 reached a constant level at the end of the experiments, in the experiments with lepidocrocite #2 and goethite the initial fast release of  $^{55}\text{Fe}$  was followed by a much slower release stage (Fig. 14). No significant release of  $^{55}\text{Fe}$  was observed in the experiments with hematite. After an initial decrease in the  $\text{Fe}^{2+}$  concentration due to adsorption onto the iron oxides, the  $\text{Fe}^{2+}$  concentration remained constant (Fig. 14). Also pH remained nearly constant during the transformation.

The distribution of bulk Fe and  $^{55}\text{Fe}$  between the aqueous and solid (including adsorbed Fe) phase at the beginning and the end of the experiments with an  $\text{Fe}^{2+}$  concentration of 0.2 and 1.0 mM is shown in Figure 15. Initially all the  $^{55}\text{Fe}$  is contained in the solid phase, but at the end of the experiments with ferrihydrite and lepidocrocite #1,  $^{55}\text{Fe}$  is distributed proportional to the bulk distribution of Fe between the aqueous and solid phase, indicating that a complete isotopic equilibration with the aqueous phase is attained. Similar results were obtained at all

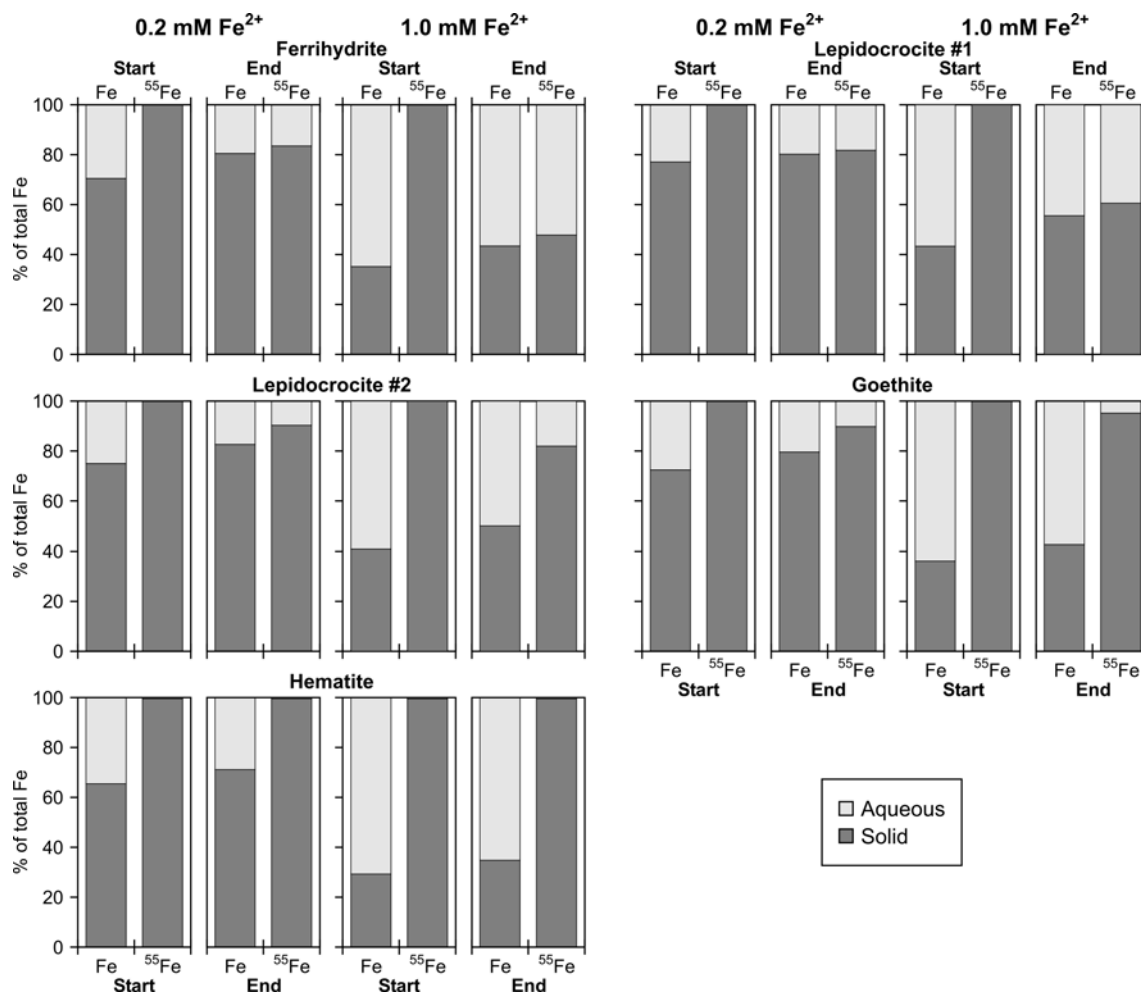


Figure 15: Distribution of bulk Fe and  $^{55}Fe$  over the aqueous and solid phases at the start and end of the experiments with ferrihydrite, the two lepidocrocites, goethite and hematite suspended in a 0.2 mM and a 1.0 mM  $Fe^{2+}$  solution. With permission from Elsevier.

the  $Fe^{2+}$  concentrations, and the plateaus of aqueous  $^{55}Fe$  in Figure 13 therefore reflect the relative pool sizes of aqueous  $Fe^{2+}$  compared to solid phase Fe(III). Isotopic equilibrium was not attained in the experiments with lepidocrocite #2 and goethite, but the slow continued  $^{55}Fe$  release at the end of the experiments (Fig. 14) indicates that isotopic equilibrium may be attained given enough time. For hematite there was no redistribution of  $^{55}Fe$  between the aqueous and solid phase.

### 5.2.1 Mechanism for $Fe^{2+}$ catalysed transformation of Fe(III) oxides

The exact mechanism of the  $Fe^{2+}$  catalysed transformation of iron oxides is not well understood. Based on the observation that magnetite, formed by the  $Fe^{2+}$  catalysed transformation of ferrihydrite, retain morphology and particle size of the ferrihydrite, a topotactic conversion of ferrihydrite to magnetite has been proposed (Ardizzone and Formaro, 1983; Fredrickson et al., 1998; Tronc et al., 1992). Other investigators

have proposed that the oxide transformation occurs via the dissolution of a precursor facilitated by the  $\text{Fe}^{2+}$  and the subsequent precipitation of the transformation product (Fischer, 1972; Tronc et al., 1992). Tronc et al. (1992) observed the existence of two stable spinel species with different morphologies and compositions after the transformation of ferrihydrite in the presence of  $\text{Fe}^{2+}$ , at Fe(II) to Fe(III) ratios of 0.1 to 0.15, and suggested that both a topotactic and a reconstructive transformation occurred simultaneously. The two processes are competitive and the kinetics of the processes are controlled by the Fe(II) level. Higher  $\text{Fe}^{2+}$  concentrations favour the reconstructive transformation and therefore the topotactic transformation only occurs at low Fe(II) to Fe(III) ratios. The release of  $^{55}\text{Fe}$  from the oxides (Figs. 13 and 14) and the attainment of isotopic equilibrium for ferrihydrite and lepidocrocite #1 (Fig. 15) found in this study support the hypothesis that  $\text{Fe}^{2+}$  facilitates the dissolution and thereby a reconstructive transformation of the iron oxides at high Fe(II) to Fe(III) ratios.

The catalysing effect of  $\text{Fe}^{2+}$  on the dissolution of Fe(III) oxides has been proposed to arise from an interfacial electron transfer from Fe(II) to Fe(III) (Fischer, 1972; Tronc et al., 1992) in a similar way as the dissolution of  $\text{Fe}_2(\text{SO}_4)_3$  by  $\text{Fe}^{2+}$  (Lieser and Schroeder, 1960) and of  $\text{CrCl}_3$  by  $\text{Cr}^{2+}$  (Cotton and Wilkinson, 1988). This mechanism involves electron exchange across the edge of the outermost octahedron of the oxide surface. However, Fe(II)-Fe(III) electron transfer is believed to occur through metal-metal bonding by overlapping d-orbitals (Sherman, 1987). The proposed electron transfer mechanism therefore requires a suitable structural rearrangement to occur (Tronc et al., 1992) which may be possible for ferrihydrite due to the amorphous structure of this iron oxide but is more questionable for more crystalline oxides. However, the reaction between  $\text{Fe}^{2+}$  and more crystalline oxides such as lepidocrocite and goethite also occurs (Fig. 14).

As an alternative mechanism, an exchange of Fe(II) for Fe(III) in the terminal octahedral positions is proposed in this study. A similar exchange has previously been described between aqueous and structural Fe(III) (Rea et al., 1994). Although the  $\text{Fe}^{2+}$  ion is larger than structural Fe(III) (0.078 nm and 0.064 nm, respectively), the ionic radius of  $\text{Fe}^{2+}$  is still close to the  $\pm 18\%$  of the radius of structural Fe(III) which is considered optimum for substitution in iron oxides (Cornell and Schwertmann, 2003).

Whether Fe(II) adheres to the surface of the oxide coupled to electron exchange or enters the crystal lattice through ion exchange followed by electron exchange, the released electron may migrate through the crystal lattice of the iron oxide (Williams and Scherer, 2004). The presence of the extra electrons decreases the stability of the crystal, and the disintegration of the oxide may subsequently release  $^{55}\text{Fe}^{2+}$  as observed in this study (Figs. 13 and 14).

The disintegration of the iron oxides is supported by a comparison of the fraction of  $^{55}\text{Fe}$  present in the outermost octahedral positions of the oxides with the fraction of  $^{55}\text{Fe}$  released to solution. From the morphology and the surface area of the iron oxide crystals, the proportion of surface sites to total sites in the crystals were estimated to constitute 25%, 24%, 10%, 5% and 3% for ferrihydrite, lepidocrocite #1 and #2, goethite and hematite, respectively (Pedersen et al., 2005). As a larger proportion of  $^{55}\text{Fe}$  is found in solution at the end of the experiments with ferrihydrite, the two

lepidocrocites and goethite (Figs. 13 and 14), the reaction between the iron oxides and  $\text{Fe}^{2+}$  cannot merely be an exchange of Fe at the surface of the iron oxides.

Hematite did not release significant amounts of  $^{55}\text{Fe}$  (Fig. 14) and only a minor fraction of the surface reacted with  $\text{Fe}^{2+}$ , even when a significant fraction of the  $\text{Fe}^{2+}$  adsorbed to the hematite surface. As the solubility constant for hematite is three orders of magnitude lower than that of ferrihydrite, one explanation could be that the high stability of hematite prevents the distortion caused by the  $\text{Fe}^{2+}$  from breaking down the crystal lattice. Another theory is that the linear arrays of octahedra containing Fe(III) found in the structure of lepidocrocite and goethite are not found in hematite.

For pyrite Rimstidt and Vaughan (2003) proposed the oxidation of pyrite to be a three step process. In the first, at an anodic site, an electron is released into the pyrite by a reaction between the oxygen atom of water and a sulphur atom in pyrite. The second step involves transport of electrons from the site of the anodic reaction to a cathodic site where electrons in a third step are transferred from the pyrite surface to the aqueous oxidant species, usually  $\text{O}_2$  or  $\text{Fe}^{3+}$ . In a similar manner, the transformation of iron oxides by the catalytic action of  $\text{Fe}^{2+}$  may involve the following steps: Adsorption of  $\text{Fe}^{2+}$  on to the oxide surface, exchange of Fe(II) for Fe(III) in the crystal lattice, electron transport to another site, and ending with the detachment of  $^{55}\text{Fe}^{2+}$ . This implies that the sites for ad- and desorption of  $\text{Fe}^{2+}$  are different and therefore must have have different energies. The driving force for the process may be the energy gradient between the ad- and desorption sites.

### 5.2.2 Kinetics of Fe(III) oxide transformation

Fischer (1972) investigated the kinetics of  $\text{Fe}^{2+}$  catalysed transformation of ferrihydrite to goethite at  $50^\circ\text{C}$  at an Fe(II)/Fe(III) ratio of 0.1 and at various pH values. The transformation of ferrihydrite to goethite was accelerated in a relative narrow pH range between pH 4 and 8, and showed a maximum at pH 6.5. The maximum acceleration of the transformation of ferrihydrite at pH 6.5 was explained by an optimum for adsorption of  $\text{Fe}^{2+}$  at this pH. While the decreased adsorption of  $\text{Fe}^{2+}$  at lower pH values was accounted for by electrostatic repulsion of the  $\text{Fe}^{2+}$  by the positively charged surface of ferrihydrite (Fig. 1), the explanation for the apparent decrease in adsorbed  $\text{Fe}^{2+}$  at higher pH is more unclear. Fischer (1972) proposed that the  $\text{Fe}^{2+}$  was inactivated either because of precipitation of  $\text{Fe}(\text{OH})_2$ , although equilibrium calculations showed the solution to be subsaturated for  $\text{Fe}(\text{OH})_2$ , or because the  $\text{Fe}^{2+}$  was oxidized to Fe(III) although tests showed that only a minor part of the  $\text{Fe}^{2+}$  was oxidized.

To investigate the pH dependence of the catalytic action of  $\text{Fe}^{2+}$  on the transformation of ferrihydrite in further detail, adsorption of  $\text{Fe}^{2+}$  onto ferrihydrite was modelled with PHREEQC (Fig. 16). These calculations seem to confirm that  $\text{Fe}^{2+}$  does not adsorb onto ferrihydrite at a pH lower than 6.5, and it is therefore reasonably to expect that in acidic solutions, the transformation of ferrihydrite is not accelerated by  $\text{Fe}^{2+}$ . In contrast, nearly all  $\text{Fe}^{2+}$  is adsorbed at a pH higher than 6.5; only at pH above 11.5 does adsorbed  $\text{Fe}^{2+}$  decrease due to precipitation of  $\text{Fe}(\text{OH})_2$ . Thus, the argument of Fischer (1972), that the accelerating effect of  $\text{Fe}^{2+}$  on the transformation of ferrihydrite was decreased at a pH higher than 6.5 due to

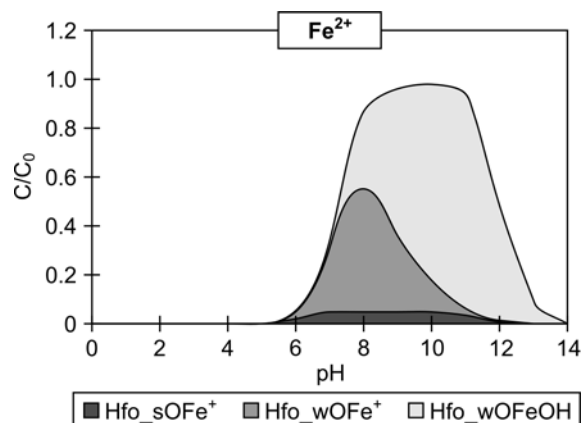


Figure 16: Adsorption of  $\text{Fe}^{2+}$  on ferrihydrite as a function of pH as calculated with PHREEQC (Parkhurst and Appelo, 1999).

precipitation of  $\text{Fe}(\text{OH})_2$  does not appear to be valid.

The mechanism proposed in this study involves the detachment of  $\text{Fe}^{2+}$ . Based on the strong sorption of  $\text{Fe}^{2+}$  onto iron oxides at alkaline pH values (Fig. 16), it is possible that at pH higher than pH 6.5 the transformation is limited by the detachment of  $\text{Fe}^{2+}$ . The transformation of ferrihydrite to magnetite has, however, been observed at room temperature at pH as high as pH 9 (Mann et al., 1989).

In this study, the effects of the  $\text{Fe}^{2+}$  concentration and the crystallinity of the iron oxide on the kinetics of the reaction between  $\text{Fe}^{2+}$  and iron oxides were investigated (Pedersen et al., 2005). For each iron oxide and  $\text{Fe}^{2+}$  concentration, the initial release rate of  $^{55}\text{Fe}$  from the oxide was calculated as the slope of a line through the first data points in Figure 13 and 14. Hematite was excluded in these calculations as no release of  $^{55}\text{Fe}$  was observed from this iron oxide (Fig. 14). To facilitate a comparison of the various rates, the rates were normalized to the total radioactivity in the oxides.

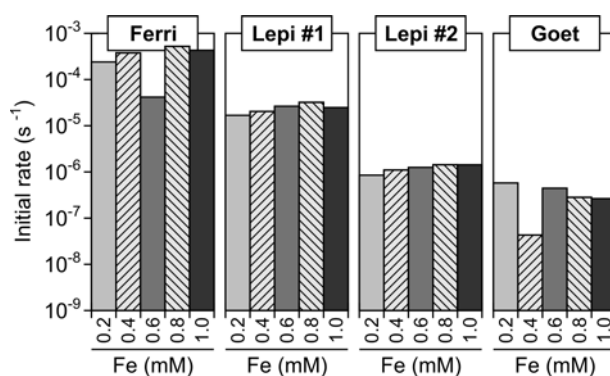


Figure 17: Initial release rate of  $^{55}\text{Fe}$  from ferrihydrite (Ferri), lepidocrocite #1 (Lepi #1) and #2 (Lepi #2), and goethite (Goet) in experiments with  $\text{Fe}^{2+}$  concentrations ranging from 0.2 to 1.0 mM. With permission from Elsevier.

The initial release rate of  $^{55}\text{Fe}$  from ferrihydrite, lepidocrocite #1 and #2, and goethite at  $\text{Fe}^{2+}$  concentrations from 0.2 to 1.0 mM is shown in Figure 17. There is

a tendency of a slightly increasing release rate with increasing  $\text{Fe}^{2+}$  concentration for all the iron oxides. However, the effect of the  $\text{Fe}^{2+}$  concentration on the initial release rate appears to be subordinate compared to the effect of mineralogy. The initial release rate of  $^{55}\text{Fe}$  decreases by approximately one order of magnitude going from ferrihydrite to lepidocrocite #1 to lepidocrocite #2 to goethite and the main control on the initial release rate appears therefore to be affiliated with the properties of the iron oxide mineral. It was unfortunately not possible to elucidate the exact properties of the iron oxides that exert the control on the  $^{55}\text{Fe}$  as, for each of the iron oxides, both the surface area and reactivity decrease and the crystal size increases as the initial release rate decreases.

### 5.2.3 Effect of adsorbed arsenate on the transformation of Fe(III) oxides

In this study, the effect of trace amounts of arsenate on the  $\text{Fe}^{2+}$  catalysed transformation of ferrihydrite and lepidocrocite was investigated (Pedersen et al., 2006). Iron oxides were coprecipitated with arsenate at As/Fe molar ratios between 0 and 0.005. The transformation was conducted at  $25^\circ\text{C}$  and at pH 6.5 as described above. To trace the transformation,  $^{55}\text{Fe}$  was incorporated congruently into the iron oxides, as shown by a congruent release of  $\text{Fe}^{2+}$  and  $^{55}\text{Fe}$  ( $r^2 = 0.982$  to  $0.999$ ) during reductive dissolution of the iron oxides in 10 mM ascorbic acid at pH 3 (Fig. 18). In the following the different iron oxides are named by the type of iron oxides (ferrihydrite or lepidocrocite) followed by the As/Fe molar ratio.

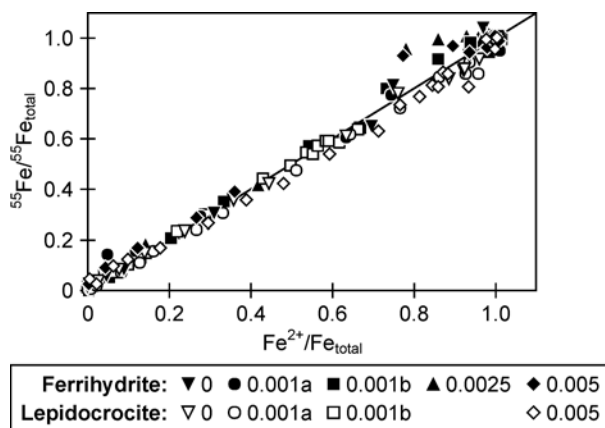


Figure 18: The release of  $^{55}\text{Fe}$  versus the release of  $\text{Fe}^{2+}$  during reductive dissolution in 10 mM ascorbic acid at pH 3 of ferrihydrite and lepidocrocite with various As/Fe molar ratios. Concentrations and activities are normalized to the added amount. The line represents congruent release.

Within 3 days, ferrihydrite transformed into lepidocrocite and goethite at the lower  $\text{Fe}^{2+}$  concentrations and into goethite and magnetite at the higher  $\text{Fe}^{2+}$  concentration, while lepidocrocite within 8 days remained unchanged at low  $\text{Fe}^{2+}$  concentrations and transformed into magnetite at the lower and higher  $\text{Fe}^{2+}$  concentrations, respectively. The same transformation products were found in the absence of

arsenate, and thus trace amounts of arsenate does not influence the transformation product of  $\text{Fe}^{2+}$  catalysed transformation of ferrihydrite and lepidocrocite.

As found previously in the absence of arsenate, the transformation of the iron oxides was accompanied by a release of  $^{55}\text{Fe}$  to solution. While isotopic equilibrium was attained in the experiments with ferrihydrite at all As/Fe molar ratios and for lepidocrocite with the As/Fe molar ratio of 0 and 0.001a, no significant redistribution of  $^{55}\text{Fe}$  was observed in the experiments with lepidocrocite 0.001b and 0.005 (Fig. 19) despite a complete transformation to magnetite. This implies a topotactic transformation of lepidocrocite to magnetite in accordance with previously reported results (Sudukar et al., 2003).

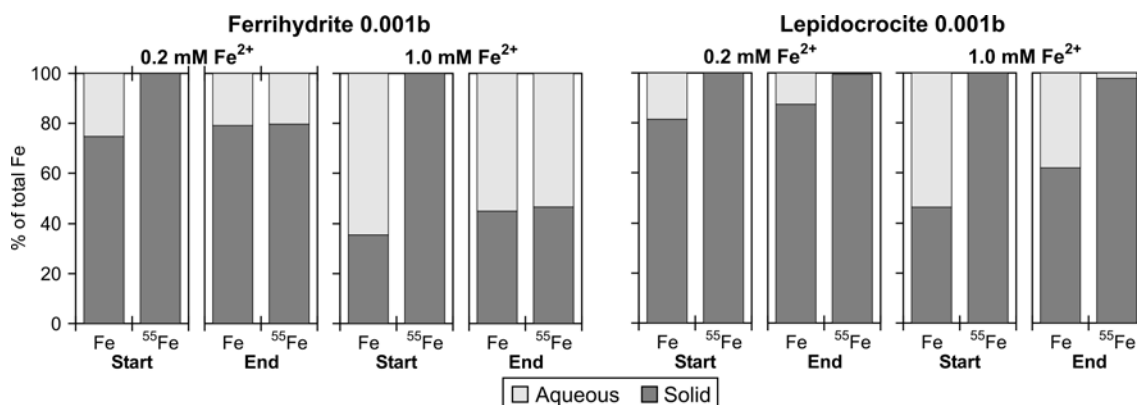


Figure 19: Distribution of bulk Fe and  $^{55}\text{Fe}$  over the aqueous and solid phases at the start and end of the experiments with ferrihydrite and lepidocrocite with the As/Fe molar ratio 0.001 suspended in a 0.2 mM and a 1.0 mM  $\text{Fe}^{2+}$  solution.

Poly-valent anions, such as silicate, phosphate and arsenate, that form strong inner sphere complexes with the iron oxide surface, are generally believed to markedly retard the transformation of ferrihydrite (Biber et al., 1994; Paige et al., 1996, 1997b; Ford, 2002). During transformation at pH 12 and 60°C of ferrihydrite coprecipitated with arsenic at molar ratios of 0.002 to 1.0, the formation of goethite was suppressed and replaced by hematite, and at As/Fe ratios of 3.0 and higher, the transformation was completely inhibited and the ferrihydrite remained amorphous (Paige et al., 1996). Similar results were found for the effect of phosphate on the recrystallization of ferrihydrite (Paige et al., 1997b). In accordance herewith Ford (2002) observed that the overall rate of ferrihydrite transformation at pH 6 and 40°C decreased with increasing arsenate loading while the rate of hematite formation increased and the rate of goethite decreased. Arsenate is believed to retard the transformation of ferrihydrite by a mechanism similar to that of hydroxyl-carboxylic acids (Sun et al., 1999) that stabilizes ferrihydrite by linking two or more units of ferrihydrite per anion thereby forming a network of particles resistant to both aggregation and dissolution (Cornell and Schwertmann, 1979).

The initial release rate of  $^{55}\text{Fe}$  during  $\text{Fe}^{2+}$  catalysed transformation of ferrihydrite at As/Fe molar ratios between 0 and 0.005 was calculated as described above and the results are shown in Figure 20. The transformation rate of ferrihydrite ap-

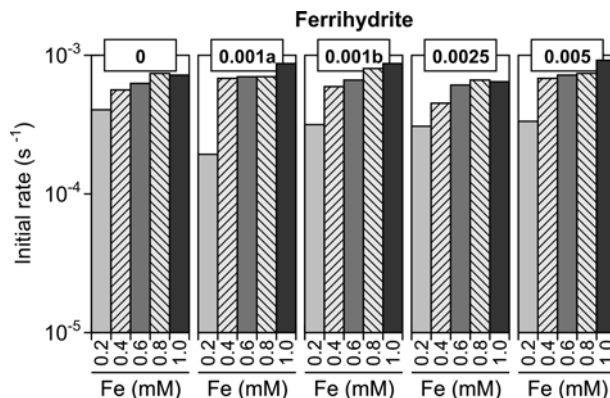


Figure 20: Initial release rate of  $^{55}\text{Fe}$  from ferrihydrite with As/Fe molar ratios between 0 and 0.005 in experiments with  $\text{Fe}^{2+}$  concentrations ranging from 0.2 to 1.0 mM.

appears to increase slightly with increasing  $\text{Fe}^{2+}$ , but appears unaffected by arsenate at As/Fe molar ratios below 0.005. Earlier studies of the effect of arsenate on the transformation of ferrihydrite show a retardation of the transformation of ferrihydrite. This discrepancy may be explained by the use of higher As/Fe molar ratios in previous studies. Furthermore, previously the transformation was induced by heating the iron oxides to  $40^\circ\text{C}$  to  $70^\circ\text{C}$  which results in rates four orders of magnitude lower than when induced by the presence of  $\text{Fe}^{2+}$ . It therefore seems reasonable to conclude, that the driving force for the transformation is stronger when induced by  $\text{Fe}^{2+}$  compared to when induced by heating.

### 5.3 The fate of adsorbed arsenate

As the transformation of ferrihydrite to lepidocrocite, goethite, hematite or magnetite is accompanied by a decrease in the surface area, it has been postulated that arsenate adsorbed to the ferrihydrite surface may desorb during the transformation (Belzile and Tessier, 1990; Dixit and Hering, 2003). However, the reversibility of the sorption process is related to the ability of the adsorbed species to become incorporated into the crystalline phase resulting from the transformation. Species like Mn(II) and Ni(II) that can substitute for Fe(III) in goethite and hematite, showed decreased sorption reversibility after the transformation of ferrihydrite to goethite and hematite, while species like Pb(II) and Cd(II) with minimal incorporation in goethite and hematite remained adsorbed to the surface of the oxides after the transformation (Ford et al., 1997).

In this study radio tracers were applied to investigate the fate of arsenate during the transformation of ferrihydrite and lepidocrocite with As/Fe molar ratios between 0 and 0.005 (Pedersen et al., 2006). To monitor the transformation of the iron oxides,  $^{55}\text{Fe}$  was incorporated congruently with the bulk of Fe into the iron oxides (Fig. 18) while  $^{73}\text{As}$  was used to trace the arsenate. Thus  $^{55}\text{Fe}$  and  $^{73}\text{As}$  were employed simultaneously as tracers. Initially all the arsenate was present as species adsorbed onto the surface of the iron oxides (Fig. 10). The fate of arsenate during the trans-



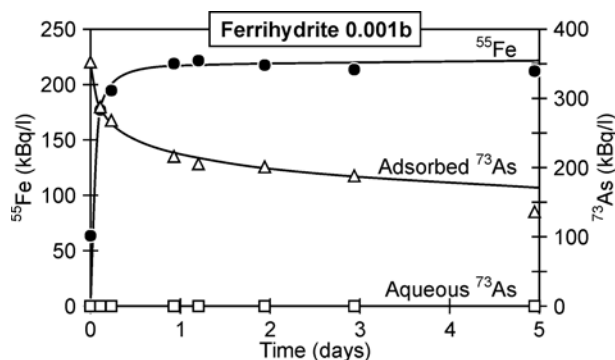


Figure 21: Aqueous  $^{55}\text{Fe}$ , adsorbed  $^{73}\text{As}$  and aqueous  $^{73}\text{As}$  during transformation of Ferrihydrite0.001b in 1.0 mM  $\text{Fe}^{2+}$ . Lines are added for visual aid.

formation was followed by determining adsorbed arsenate by extraction of the  $^{73}\text{As}$  with a 250  $\mu\text{M}$  arsenate solution as previously described. The transformation was conducted in the presence of  $\text{Fe}^{2+}$  at 25°C and pH 6.5 as described above.

As the activity of aqueous  $^{55}\text{Fe}$  increases during the transformation of ferrihydrite, the activity of desorbable arsenic decreases and after 3 days only 45% of the arsenic remains desorbable (Fig. 21). The concentration of aqueous arsenic remains insignificant compared to that of desorbable arsenic which is exclusively present as arsenate.

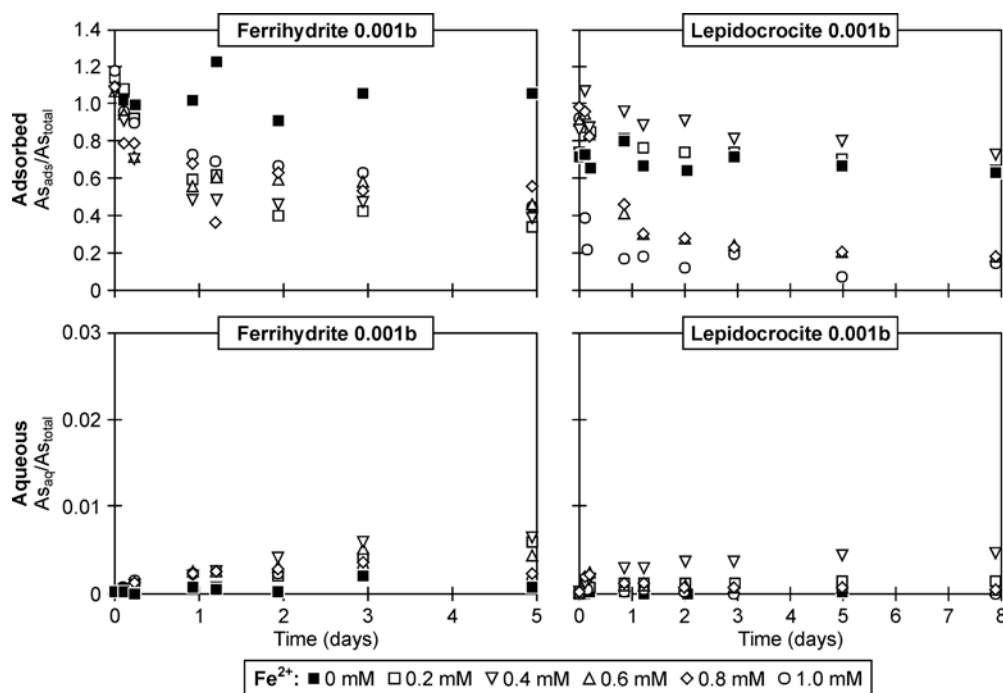


Figure 22: Adsorbed (top) and aqueous (bottom)  $^{73}\text{As}$  during the transformation of Ferrihydrite0.001b (left) and Lepidocrocite0.001b (right) in  $\text{Fe}^{2+}$  concentrations ranging from 0 to 1.0 mM.

Figure 22 shows the activity of adsorbed and aqueous  $^{73}\text{As}$  during the transformation of Ferrihydrite0.001b and Lepidocrocite0.001b at various  $\text{Fe}^{2+}$  concentrations. In the absence of  $\text{Fe}^{2+}$  for both ferrihydrite and lepidocrocite and at the lowest  $\text{Fe}^{2+}$  concentrations for lepidocrocite, desorbable arsenic remains constant, while desorbable arsenic generally decreases with time when  $\text{Fe}^{2+}$  is present. The decrease in desorbable arsenic is correlated with a transformation of ferrihydrite and lepidocrocite to more crystalline phases or magnetite.

Less than 1% of the total arsenate is released to the solution during the transformation (Fig. 22) and the observed decrease in desorbable arsenic is therefore not accompanied by a corresponding increase in aqueous arsenic. Instead arsenic apparently becomes bound more strongly to the iron oxides. The small amount of arsenic that is released during transformation is present as arsenite, and some of the arsenate originally adsorbed onto the surface of the oxides must become reduced to arsenite prior to its release.

Earlier investigations of the fate of arsenate during the transformation of ferrihydrite have contrasting conclusions. Paige et al. (1994, 1996) concluded that arsenate is not incorporated into the more crystalline phases, since XRD and X-ray fluorescence spectroscopy of the transformation product of ferrihydrite showed no evidence of arsenic containing phases. Similar results have been found for phosphate (Paige et al., 1997b). In contrast, Sun et al. (1999) and Ford (2002) used extraction techniques to localize the arsenate after the transformation of ferrihydrite to goethite and hematite and concluded that arsenate is incorporated into the more crystalline phases. The results presented here, provide more direct evidence concerning the incorporation of arsenate during the transformation of ferrihydrite and lepidocrocite because the use of radio tracers enables a speciation between adsorbed arsenic and arsenic incorporated in the crystal.

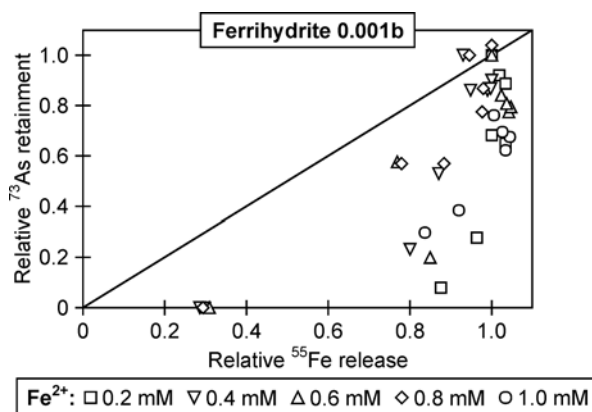


Figure 23: The relative incorporation of  $^{73}\text{As}$  as a function of the relative release of  $^{55}\text{Fe}$  from Ferrihydrite0.001b in  $\text{Fe}^{2+}$  concentrations ranging from 0.2 to 1.0 mM. The line represents equal rates of incorporation of  $^{73}\text{As}$  and release of  $^{55}\text{Fe}$ .

The relative incorporation of  $^{73}\text{As}$  into the transformation products versus the relative release of  $^{55}\text{Fe}$  is displayed in Figure 23. Using the release of  $^{55}\text{Fe}$  as an indicator for the extent of the transformation of ferrihydrite, Figure 23 demonstrates

that the incorporation of  $^{73}\text{As}$  into the crystalline product primarily occurs during the final stage of the transformation. This may be because arsenate remains preferentially adsorbed onto the ferrihydrite until the surface of ferrihydrite becomes too small to contain all the arsenic in adsorbed form.

## 6 Discussion

### 6.1 $\text{Fe}^{2+}$ catalysed transformation of Fe(III) oxides

Although the transformation of ferrihydrite and lepidocrocite to more crystalline Fe(III) oxides phases or magnetite in the presence of  $\text{Fe}^{2+}$  has been observed by several investigators as early as in 1967 (van Oosterhout, 1967), the implications of this process does not appear to be widely acknowledged. Traditionally, iron oxides are considered as phases having a constant composition with respect to characteristics such as sorption capacity and reduction rates. However, due to the rapid transformation of the least stable iron oxides in the presence of  $\text{Fe}^{2+}$ , the iron oxides instead become dynamic phases and this should be taken into account when studying the iron pool under reducing conditions.

A field of research where the transformation of ferrihydrite and lepidocrocite is of great importance is the modelling of sorption of trace metals and oxyanions, such as arsenate and phosphate, on iron oxides in transitional oxidized-reduced environments. Most models, such as the widely applied surface complexation model for ferrihydrite (Dzombak and Morel, 1990; Appelo et al., 2002) consider the sorption capacity of the solid phase as a constant, only related to the amount present. However, if the sorbing solid phase changes due to  $\text{Fe}^{2+}$  induced transformations, the model becomes invalid, as the sorption capacity decreases leading to a desorption of the adsorbed species. Alternatively, the adsorbed species may be incorporated into the newly formed more crystalline phase and become inactivated with respect to desorption and ion exchange. Furthermore, the significance of  $\text{Fe}^{2+}$  adsorption experiments on various iron oxides (Liger et al., 1999) and the applicability of  $\text{Fe}^{2+}$  adsorption models (Fig. 16) (Appelo et al., 2002) is highly questionable and should only be used tentatively.

In natural environments, iron oxides are present as a mixture of several minerals of which ferrihydrite, lepidocrocite, goethite and hematite are the most common. Ferrihydrite is considered to be the most important iron phase for microbial iron reduction in sediments (Lovley, 1992; Thamdrup, 2000) as well as for abiotic reduction by sulphide in marine environments (Poulton et al., 2004). The  $\text{Fe}^{2+}$  initially produced during the reduction of ferrihydrite could cause an autocatalytic transformation of the remainder of the ferrihydrite and the other iron oxides into less reactive phases. Such a transformation would decrease the reactivity of the iron pool thereby decreasing or even terminating further bioreduction. The crystal structure and particle size of the transformation product appears to be controlled by the adsorption density and supply kinetics of biogenic  $\text{Fe}^{2+}$ . Lepidocrocite, goethite and hematite are formed from ferrihydrite when ferrihydrite is in great excess compared to the electron donor, while a lower electron donor to acceptor ratio leads to small particle-size lepidocrocite and goethite, and finally when the electron donor is in excess, ferrihydrite is transformed into fine-grained magnetite (Zachara et al., 2002).

Freshwater environments with ongoing iron oxide reduction are traditionally rich in  $\text{Fe}^{2+}$ , whereas  $\text{Fe}^{2+}$  is expected to precipitate with the high dissolved sulphide concentrations found in many marine environments.  $\text{Fe}^{2+}$  may therefore become inactivated in marine environments and therefore perhaps not catalyse the transformation

of the least stable iron oxides to the same extent as in freshwater environments. Recent studies (Poulton, 2003; Poulton et al., 2004) show, however, that a significant proportion of the  $\text{Fe}^{2+}$  produced during iron reduction by sulphide remains associated with the oxide surface for a considerable period of time. These observations suggest that  $\text{Fe}^{2+}$  catalysed transformation of iron oxides may also be of potential importance in sulphidic environments. However, Fischer (1972) observed a significant decrease in the  $\text{Fe}^{2+}$  catalysed transformation of ferrihydrite at pH higher than 6.5, and at the pH range of most marine waters (7.5 -8.5) only a minor fraction of the ferrihydrite should become transformed. On the other hand, the transformation of both ferrihydrite and lepidocrocite have been observed at pH values as high as 9 (Tamura et al., 1983; Cornell and Schneider, 1989; Mann et al., 1989).

The solubility of iron oxides has been estimated by simultaneous determination of pe, pH and the activity of aqueous  $\text{Fe}^{2+}$  in suspensions of the iron oxide to which soluble  $\text{Fe}^{2+}$  has been added (Bonneville et al., 2004). The solutions were allowed to equilibrate for 3-4 hours during which a significant proportion of the ferrihydrite and lepidocrocite are expected to transform (Figs. 13 and 14). For the solubility determinations, the redox potential measurement is controlled by the most reactive phase in the system (Ardizzone and Formaro, 1983) since this phase controls the activity of aqueous  $\text{Fe}^{3+}$  at equilibrium. However, at a given time, the most reactive fraction of the iron oxide is expected to transform. The solubility found by Bonneville et al. (2004) must therefore reflect the solubility of the fraction of ferrihydrite that has not transformed at the time of determination and not the original iron oxide.

The field of stable iron isotope studies is rapidly expanding, and stable iron isotopes have been applied to trace biogeochemical iron fluxes and iron redox changes (Beard and Johnson, 2003). For example, a significant (1.3‰) Fe-isotopic fractionation during dissimilatory iron reduction has been observed (Beard et al., 1999; Icopini et al., 2004) and stable Fe isotopic compositions have therefore been suggested as indicators for microbial activity in the early history of the earth (Beard et al., 1999). The isotopic re-equilibration caused by iron oxide transformations observed in this study (Fig. 15) suggest that the interpretation of stable Fe isotope signatures should be done with care.

All studies of the  $\text{Fe}^{2+}$  catalysed transformation of iron oxides carried out so far are simple laboratory experiments with solutions containing a synthetic iron oxide and aqueous  $\text{Fe}^{2+}$  and in some studies a buffer. In experiments with bioreduction of the iron oxides a bacterial medium is also present. The chemistry of natural sediments is much more complex and one should be careful in transferring the conclusions of this study to natural sediments. For example, natural sediments contain a large range of other compounds such as organics, phosphorus, aluminium and silica, that may inhibit the transformation of the iron oxides (Cornell and Schwertmann, 1979; Galvez et al., 1999; Schwertmann et al., 2000; Campbell et al., 2002; Alvarez et al., 2005). However,  $\text{Fe}^{2+}$  catalysed transformation of iron oxides may in principle also occur in some sediments and the process should therefore be kept in mind when interpreting data from the transitional oxidized reduced zone of natural sediments.

## 6.2 The fate of arsenic

Several studies have shown that arsenate coprecipitated with ferrihydrite (Fuller et al., 1993; Waychunas et al., 1993, 1996; Pedersen et al., 2006) and lepidocrocite (Pedersen et al., 2006) mainly associates with the iron oxide surface. Compared to arsenate incorporated in the crystal structure, arsenate associated with the iron oxide surface may be more susceptible to reactions releasing the arsenate to the solution. For example, adsorbed arsenic may be mobilized by competitive anion exchange with phosphate from fertilizers (Acharyya et al., 1999, 2000; Schwartz et al., 2004), with carbonate derived from oxidation of organic matter (Appelo et al., 2002; Anawar et al., 2004) or with organic matter (Redman et al., 2002). Adsorbed arsenate may also be released upon reductive dissolution of the iron oxides as the available surface area decreases (Nickson et al., 2000; McArthur et al., 2001; Kinniburgh and Smedley, 2001; Bose and Sharma, 2002; Schwartz et al., 2004; Pedersen et al., 2006). Furthermore, the reduction of adsorbed arsenate to arsenite may under certain conditions result in a release of arsenic to solution (Ahmann et al., 1997; Zobrist et al., 2000; Dixit and Hering, 2003).

In the metallurgical industry, two technologies are presently applied for the removal of arsenic; coprecipitation of arsenic with ferrihydrite and the precipitation of crystalline scorodite ( $\text{FeAsO}_4 \cdot \text{H}_2\text{O}$ ) (Twidwell et al., 2005). Despite the higher stability of scorodite as compared to ferrihydrite (Welham et al., 2000; Cornell and Schwertmann, 2003), the precipitation of ferrihydrite is commonly preferred (Twidwell et al., 2005; Harris, 2000), as this technology is more cost efficient compared to the requirement of temperatures near  $100^\circ\text{C}$  for scorodite precipitation. Arsenic is also often removed in sand filters at water works from drinking water by the precipitation with or adsorption on ferrihydrite (Jessen et al., 2005). The long term stability of ferrihydrite is, however, a matter of concern. The presence of commonly associated metals (Co, Pb and Zn) may have a stabilizing effect on the long term stability of ferrihydrite from the metallurgical industry, and the association of arsenate with the oxide surface means that arsenate may readily be released by ion exchange.

The transformation of ferrihydrite and lepidocrocite to more crystalline Fe(III) oxide phases or magnetite results in the incorporation of arsenate into the crystalline structure (Fig. 22). This may reduce the arsenate susceptibility to become released, in part by inhibiting the arsenate to take part in anion exchange reactions as well as the reduction to arsenite on the oxide surface and in part by lowering the reduction rate of the iron oxide pool. The transformation of ferrihydrite and lepidocrocite, to which arsenate is adsorbed, into more stable Fe(III) oxides may therefore be an important trapping mechanism for arsenate in natural sediments.

The reduction of iron oxides has been suggested as a mechanism for arsenic release in Bangladesh (Nickson et al., 2000; Bose and Sharma, 2002; Horneman et al., 2004; van Geen et al., 2004). The reductive dissolution experiments conducted in this study imply that a congruent release of arsenate with iron cannot be expected upon reduction of the iron oxides. While arsenate is repelled from lepidocrocite, arsenate adsorbs strongly onto ferrihydrite and goethite. This may in part explain the partial decoupling of the arsenic and the iron concentrations observed in groundwater data from Bangladesh (Nickson et al., 2000; Mandal and Suzuki, 2002); samples high

in arsenic may be low in iron and visa verse. Further mechanisms decoupling the dissolved arsenate and iron concentration include the release of arsenic without iron dissolution, and reprecipitation or readsorption of  $\text{Fe}^{2+}$  (Horneman et al., 2004; van Geen et al., 2004). In natural sediments it may therefore be very difficult to predict the release of arsenate during reductive dissolution of iron oxides.

## 7 Conclusions

There occurs an immediate and rapid reaction between dissolved  $\text{Fe}^{2+}$  and iron oxides. In the presence of  $\text{Fe}^{2+}$ , ferrihydrite transformed completely into lepidocrocite and goethite within two days. Within this time frame, a complete isotopic equilibration between the aqueous and solid phases was attained. This implies a recrystallization of solid Fe(III) phases induced by the catalytic action of aqueous Fe(II). Accordingly, iron oxides should properly be considered as dynamic phases that change characteristics, such as sorption capacity and reduction rate, in transitional oxidising and reducing environments. These results have important implications for modelling the sorption of trace metals and oxyanions on iron oxides under variable redox conditions. Furthermore, the isotopic exchange between solid and solution during the transformation of iron oxides should be taken into account in the interpretation of stable iron isotopic signatures.

Coprecipitation of arsenate with ferrihydrite and lepidocrocite appeared to be an inadequate long term disposal mechanism of arsenate since the arsenate remained associated with the iron oxide surface from where it may easily become released again to solution. A transformation, by the catalytic action of  $\text{Fe}^{2+}$ , of the iron oxides to which the arsenate is adsorbed may, however, immobilize the arsenate since a significant proportion of the arsenate is incorporated into the newly formed crystalline structure. The rate of  $\text{Fe}^{2+}$  catalysed transformation of ferrihydrite and lepidocrocite was unaffected by the association of trace amounts of arsenate (As/Fe molar ratios less than 0.005) with the iron oxide surface as was the reactivity of ferrihydrite, lepidocrocite and goethite towards reductive dissolution in 10 mM ascorbic acid at pH 3. Upon reduction of the iron oxides, arsenate remains preferentially adsorbed on ferrihydrite and goethite until the surface area become too small to retain all the arsenate while arsenate is immediately released from lepidocrocite.

The use of radio tracers proved to be an easily accessible and useful tool providing important information on the reaction mechanisms involved that would otherwise be difficult to obtain. For example, the use of radio tracers enabled the direct measurement of the kinetics of the  $\text{Fe}^{2+}$  catalysed transformation of the iron oxides and gave insight into the mechanism of the reaction between  $\text{Fe}^{2+}$  and the iron oxides. The release of  $^{55}\text{Fe}^{2+}$  to the solution during the transformation of the iron oxides provided direct evidence for the electron transport from one site to another within the iron oxides. Furthermore, the radio tracers allowed a determination of the distribution of arsenate between the aqueous, adsorbed and firmly bound phases during the reductive dissolution and transformation of the iron oxides.





## References

- Acharyya, S., Chakraborty, P., Lahiri, S., Raymahashay, B. C., Guha, S., and Bhowmik, A. (1999). Arsenic poisoning in the Ganges delta. The natural contamination of drinking water by arsenic needs to be urgently addressed. *Nature*, 401:545–547.
- Acharyya, S. K., Lahiri, S., Raymahashay, B. C., and Bhowmik, A. (2000). Arsenic toxicity of groundwater in parts of the Bengal basin in India and Bangladesh. The role of Quaternary stratigraphy and Holocene sea-level fluctuation. *Environmental Geology*, 39:1127–1137.
- Afonso, M. D. S., Morando, P. J., Blesa, M. A., Banwart, S., and Stumm, W. (1990). The reductive dissolution of iron oxides by ascorbate: The role of carboxylate anions in accelerating reductive dissolution. *Journal of Colloid and Interface Science*, 138:74–82.
- Ahmann, D., Krumholz, L. R., Hemond, H. F., Lovley, D. R., and Morel, F. M. M. (1997). Microbial mobilization of arsenic from sediments of the Aberjona watershed. *Environmental Science & Technology*, 31:2923–2930.
- Albrechtsen, H.-J. and Christensen, T. H. (1994). Evidence for microbial iron reduction in a landfill leachate-polluted aquifer (Vejen, Denmark). *Applied and Environmental Microbiology*, 60:3920–3925.
- Alvarez, M., Sileo, E. E., and Rueda, E. H. (2005). Effect of Mn(II) incorporation on the transformation of ferrihydrite to goethite. *Chemical Geology*, 216:89–97.
- Anawar, H. M., Akai, J., and Sakugawa, H. (2004). Mobilization of arsenic from subsurface sediments by effect of bicarbonate ions in groundwater. *Chemosphere*, 54:753–762.
- Appelo, C. A. J. and Postma, D. (2005). *Geochemistry, Groundwater and Pollution*. A. A. Balkema, 2<sup>nd</sup> edition.
- Appelo, C. A. J., van der Weiden, M. J. J., Tournassat, C., and Charlet, L. (2002). Surface complexation of ferrous iron and carbonate on ferrihydrite and the mobilization of arsenic. *Environmental Science & Technology*, 36:3096–3103.
- Ardizzone, S. and Formaro, L. (1983). Temperature induced phase transformation of metastable Fe(OH)<sub>3</sub> in the presence of ferrous ions. *Materials Chemistry and Physics*, 8:125–133.
- Ballesteros, M. C., Rueda, E. H., and Blesa, M. A. (1998). The influence of iron (II) and (III) on the kinetics of goethite dissolution by EDTA. *Journal of Colloid and Interface Science*, 201:13–19.
- Banwart, S., Davies, S., and Stumm, W. (1989). The role of oxalate in accelerating the reductive dissolution of hematite ( $\alpha$ -Fe<sub>2</sub>O<sub>3</sub>) by ascorbate. *Colloids and Surfaces*, 39:303–309.
- Beard, B. L. and Johnson, C. M. (2003). High and low temperature applications of Fe isotope geochemistry. *The Geochemical News*, 117:8–13.
- Beard, B. L., Johnson, C. M., Cox, L., Sun, H., Neelson, K. H., and Aguilar, C. (1999). Iron isotope biosignatures. *Science*, 285:1889–1892.
- Belzile, N. and Tessier, A. (1990). Interactions between arsenic and iron oxyhydroxides in lacustrine sediments. *Geochimica et Cosmochimica Acta*, 54:103–109.
- Biber, M. V., Afonso, M. D. S., and Stumm, W. (1994). The coordination-chemistry

- of weathering: IV. Inhibition of dissolution of oxide minerals. *Geochimica et Cosmochimica Acta*, 58:1999–2010.
- Bondietti, G., Sinniger, J., and Stumm, W. (1993). The reactivity of Fe(III) (hydr)oxides: Effects of ligands in inhibiting the dissolution. *Colloids and Surfaces A: Physicochemical and Engineering Aspects*, 79:157–167.
- Bonneville, S., van Cappellen, P., and Behrends, T. (2004). Microbial reduction of iron(III) oxyhydroxides: Effects of mineral solubility and availability. *Chemical Geology*, 212:255–268.
- Bose, P. and Sharma, A. (2002). Role of iron in controlling speciation and mobilization of arsenic in subsurface environment. *Water Research*, 36:4916–4926.
- Campbell, A. S., Schwertmann, U., Stanjek, H., Friedl, J., Kyek, A., and Campbell, P. A. (2002). Si incorporation into hematite by heating Si-ferrihydrite. *Langmuir*, 18:7804–7809.
- Canfield, D. E., Raiswell, R., and Bottrell, S. (1992). The reactivity of sedimentary iron minerals toward sulfide. *American Journal of Science*, 292:659–683.
- Carlson, L., Bigham, J. M., Schwertmann, U., Kyek, A., and Wagner, F. (2002). Scavenging of As from acid mine drainage by schwertmannite and ferrihydrite: A comparison with synthetic analogues. *Environmental Science & Technology*, 36:1712–1719.
- Christoffersen, J. and Christoffersen, M. R. (1976). The kinetics of dissolution of calcium sulphate dihydrate in water. *Journal of Crystal Growth*, 35:79–88.
- Clausen, L., Fabricius, I., and Madsen, L. (2001). Adsorption of pesticides onto quartz, calcite, kaolinite and  $\alpha$ -alumina. *Journal of Environmental Quality*, 30:846–857.
- Cornell, R. M. and Schneider, W. (1989). Formation of goethite from ferrihydrite at physiological pH under the influence of cysteine. *Polydron*, 8:149–155.
- Cornell, R. M. and Schwertmann, U. (1979). Influence of organic anions on the crystallization of ferrihydrite. *Clays and Clay Minerals*, 27:402–410.
- Cornell, R. M. and Schwertmann, U. (2003). *The iron oxides: Structure, properties, reactions, occurrences and uses*. WILEY-VCH Verlag GmbH & Co., 2<sup>nd</sup> edition.
- Cotton, F. A. and Wilkinson, G. (1988). *Advanced inorganic chemistry*. John Eiley & Sons, 5<sup>th</sup> edition.
- Das, A. and Caccavo, F. J. (2000). Dissimilatory Fe(III) oxide reduction by *Shewanella alga* BrY requires adhesion. *Current Microbiology*, 40:344–347.
- Das, D., Samata, G., Mandal, B. K., Chowdhury, T. R., Chanda, C. R., Chowdhury, P. P., Basu, G. K., and Chakraborti, D. (1996). Arsenic in groundwater in six districts of West Bengal, India. *Environmental Geochemistry and Health*, 18:5–15.
- Dixit, S. and Hering, J. G. (2003). Comparison of arsenic(V) and arsenic(III) sorption onto iron oxide minerals: Implications for arsenic mobility. *Environmental Science & Technology*, 37:4182–4189.
- dos Santos Afonso, M. and Stumm, W. (1992). Reductive dissolution of iron(III) (hydr)oxides by hydrogen sulfide. *Langmuir*, 8:1671–1675.
- Drits, V. A., Sakharov, B. A., Salyn, A. L., and Manceau, A. (1993). Structural model for ferrihydrite. *Clay Minerals*, 28:185–207.
- Dzombak, D. A. and Morel, F. M. M. (1990). *The generalized two-layer model*. John

- Wiley & Sons, Inc.
- Eick, M. J., Peak, J. D., and Brady, W. D. (1999). The effect of oxyanions on the oxalate-promoted dissolution of goethite. *Soil Science Society of America Journal*, 63:1133–1141.
- Farquhar, M. L., Charnock, J. M., Livens, F. R., and Vaughan, D. J. (2002). Mechanisms of arsenic uptake from aqueous solution by interaction with goethite, lepidocrocite, mackinawite, and pyrite: An X-ray absorption spectroscopy study. *Environmental Science & Technology*, 36:1757–1762.
- Fendorf, S., Eick, M. J., Grossl, P., and Sparks, D. L. (1997). Arsenate and chromate retention mechanisms on goethite 1. Surface structure. *Environmental Science & Technology*, 31:315–320.
- Ferdelman, T. G., Lee, C., Pantoja, S., Harder, J., Bebout, B. M., and Fossing, H. (1997). Sulfate reduction and methanogenesis in a Thioploca-dominated sediment off the coast of Chile. *Geochimica et Cosmochimica Acta*, 61:3065–3079.
- Fischer, W. R. (1972). Die Wirkung von zweiwertigem Eisen auf Lösung und Umwandlung von Eisen(III)-hydroxiden. *Pseudogley and Gley. Trans. Comm. V & VI Int Sci. Soc.*, pages 37–44.
- Ford, R. G. (2002). Rates of hydrous ferric oxide crystallization and the influence on coprecipitated arsenate. *Environmental Science & Technology*, 36:2459–2463.
- Ford, R. G., Bertsch, P. M., and Farley, K. J. (1997). Changes in transition and heavy metal partitioning during hydrous iron oxides aging. *Environmental Science & Technology*, 31:2028–2033.
- Fredrickson, J. K., Zachara, J. M., Kennedy, D. W., Dong, H., Onstott, T. C., Hinman, N. W., and Li, S. (1998). Biogenic iron mineralization accompanying the dissimilatory reduction of hydrous ferric oxide by a groundwater bacterium. *Geochimica et Cosmochimica Acta*, 62:3239–3257.
- Fuller, C. C., Davis, J. A., and Waychunas, G. A. (1993). Surface chemistry of ferrihydrite: Part 2. Kinetics of arsenate adsorption and coprecipitation. *Geochimica et Cosmochimica Acta*, 57:2271–2282.
- Galvez, N., Barron, V., and Torrent, J. (1999). Preparation and properties of hematite with structural phosphorus. *Clays and Clay Minerals*, 47:375–385.
- Goldberg, S. (2002). Competitive adsorption of arsenate and arsenite on oxides and clay minerals. *Soil Science Society of America Journal*, 66:413–421.
- Goldberg, S. and Johnston, C. T. (2001). Mechanisms of arsenic adsorption on amorphous oxides evaluated using macroscopic measurements, vibrational spectroscopy, and surface complexation modeling. *Journal of Colloid and Interface Science*, 234:204–216.
- Grossl, P., Eick, M. J., Sparks, D. L., Goldberg, S., and Ainsworth, C. C. (1997). Arsenate and chromate retention mechanisms on goethite. 2. Kinetic evaluation using a pressure-jump relaxation technique. *Environmental Science & Technology*, 31:321–326.
- Grossl, P. R. and Sparks, D. L. (1995). Evaluation of contaminant ion adsorption/desorption on goethite using pressure-jump relaxation kinetics. *Geoderma*, 67:87–101.
- Hansel, C. M., Benner, S. G., Neiss, J., Dohnalkova, A., Kukkadapu, R. K., and

- Fendorf, S. (2003). Secondary mineralization pathways induced by dissimilatory iron reduction of ferrihydrite under advective flow. *Geochimica et Cosmochimica Acta*, 67:2977–2992.
- Hansen, L. K., Jakobsen, R., and Postma, D. (2001). Methanogenesis in a shallow sandy aquifer, Rømø, Denmark. *Geochimica et Cosmochimica Acta*, 65:2925–2935.
- Harris, G. B. (2000). *Minor elements 2000, processing and env. aspects of As, Sb, Se, Te, and Bi*, chapter The removal and stabilization of arsenic from aqueous proces solutions: Past, present, and future, pages 3–21. Littleton, CO: Society of mining, metallurgy and exploration, Inc., SME.
- Hering, J. G. and Stumm, W. (1990). *Mineralogical society of America*, chapter Oxidative and reductive dissolution of minerals, pages 427–465. Mineralogical Society of America.
- Horneman, A., van Geen, A., Kent, D. V., Mathe, P. E., Zheng, Y., Dhar, R. K., O’Connell, S., Hoque, M. A., Aziz, Z., Shamsudduha, M., Seddique, A. A., and Ahmed, K. M. (2004). Decoupling of As and Fe release to Bangladesh groundwater under reducing conditions. Part I. Evidence from sediment profiles. *Geochimica et Cosmochimica Acta*, 68:3459–3473.
- Hsai, T., Lo, S., Lin, C., and Lee, D. (1994). Characterization of arsenate adsorption on hydrous iron oxide using chemical and physical methods. *Colloids and Surfaces A: Physicochemical and Engineering Aspects*, 85:1–7.
- Icopini, G. A., Anbar, A. D., Ruebush, S. S., Tien, M., and Brantley, S. L. (2004). Iron isotope fractionation during microbial reduction of iron: The importance of adsorption. *Geology*, 32:205–208.
- Jackson, L. J. (1998). Paradigms of metal accumulation in rooted aquatic vascular plants. *The Science of the Total Environment*, 219:223–231.
- Jain, A., Raven, K. P., and Loeppert, R. H. (1999). Arsenite and arsenate adsorption on ferrihydrite: Surface charge reduction and net OH<sup>-</sup> release stoichiometry. *Environmental Science & Technology*, 33:1179–1184.
- Jakobsen, R. and Postma, D. (1999). Redox zoning, rates of sulfate reduction and interactions with Fe-reduction and methanogenesis in a shallow aquifer, Rømø, Denmark. *Geochimica et Cosmochimica Acta*, 63:137–151.
- Jambor, J. L. and Dutrizac, J. E. (1998). Occurrence and constitution of natural and synthetic ferrihydrite, a widespread iron oxyhydroxide. *Chemical Review*, 98:2549–2585.
- Jang, J., Dempsey, B. A., Catchen, G. L., and Burgos, W. D. (2003). Effects of Zn(II), Cu(II), Mn(II), Fe(II), NO<sub>3</sub><sup>-</sup>, or SO<sub>4</sub><sup>2-</sup> at pH 6.5 and 8.5 on transformations of hydrous ferric oxide (HFO) as evidenced by Mössbauer spectroscopy. *Colloids and Surfaces A: Physicochemical and Engeneering Aspects*, 221:55–68.
- Janney, D. E., Cowley, J. M., and Buseck, P. R. (2000). Structure of synthetic 2-line ferrihydrite by electron nanodiffraction. *American Mineralogist*, 85:1180–1187.
- Jeon, B., Dempsey, B. A., and Burgos, W. D. (2003). Kinetics and mechanisms for reactions of Fe(II) with iron(III) oxides. *Environmental Science & Technology*, 37:3309–3315.
- Jeon, B., Dempsey, B. A., Burgos, W. D., and Royer, R. A. (2001). Reactions of ferrous iron with hematite. *Colloids and Surfaces A: Physicochemical and*

- Engeneering Aspects*, 191:41–55.
- Jessen, S., Larsen, F., Koch, C. B., and Arvin, E. (2005). Sorption and desorption of arsenic to ferrihydrite in a sand filter. *Environmental Science & Technology*, 39:8045–8051.
- Jolivet, J., Belleville, P., Tronc, E., and Livage, J. (1992). Influence of Fe(II) on the formation of the spinel iron oxide in alkaline medium. *Clays and Clay Minerals*, 40:531–539.
- Jørgensen, B. B. (1978). A comparison of methods for the quantification of bacterial sulfate reduction in coastal marine sediments. *Geomicrobiology Journal*, 1:11–27.
- Kinniburgh, D. G. and Smedley, P. L. (2001). Arsenic contamination of groundwaters in Bangladesh, Vol 1: Summary. Technical report, WC/00/19, British Geological Survey.
- Kostka, J. E. and Nealson, K. H. (1995). Dissolution and reduction of magnetite by bacteria. *Environmental Science & Technology*, 29:2535–2540.
- Larsen, O. and Postma, D. (2001). Kinetics of reductive bulk dissolution of lepidocrocite, ferrihydrite, and goethite. *Geochimica et Cosmochimica Acta*, 65:1367–1379.
- Lieser, K. H. and Schroeder, H. (1960). Die Kinetik der Auflösung des wasserfreie Eisen(III)-sulfats in Eisen(II)-ionen-haltigen Lösungen. *Zeitschrift für Elektrochemie*, 64:252–257.
- Liger, E., Charlet, L., and van Cappellen, P. (1999). Surface catalysis of uranium(VI) reduction by iron(II). *Geochimica et Cosmochimica Acta*, 63:2939–2955.
- Lonergan, D. J., Jenter, H. L., Coates, J. D., Phillips, E. J. P., Schmidt, T. M., and Lovley, D. R. (1996). Phylogenetic analysis of dissimilatory Fe(III)-reducing bacteria. *Journal of Bacteriology*, 178:2402–2408.
- Lovley, D. R. (1992). Microbial oxidation of organic matter coupled to the reduction of Fe(III) and Mn(IV) oxides. *Catena Supplement*, 21:101–114.
- Lovley, D. R. (1997). Microbial Fe(III) reduction in subsurface environments. *FEMS Microbiology Ecology*, 20:305–313.
- Lovley, D. R. (2000). *Subsurface Microbiology and Biogeochemistry*, chapter Reduction of iron and humics in subsurface environments, pages 193–217. John Wiley & Sons, Inc.
- Lovley, D. R., Coates, J. D., Blunt-Harris, E. L., Phillips, E. J. P., and Woodward, J. C. (1996). Humic substances as electron acceptors for microbial respiration. *Nature*, 382:445–448.
- Lovley, D. R. and Phillips, E. J. P. (1988). Novel mode of microbial energy metabolism: Organic carbon oxidation coupled to dissimilatory reduction of iron or manganese. *Applied and Environmental Microbiology*, 54:1472–1480.
- Lovley, D. R., Phillips, E. J. P., and Lonergan, D. J. (1991). Enzymatic versus nonenzymatic mechanisms for Fe(III) reduction in aquatic sediments. *Environmental Science Technology*, 25:1062–1067.
- Luu, Y. and Ramsay, J. A. (2003). Review: Microbial mechanisms of accessing insoluble Fe(III) as an energy source. *World Journal of Microbiology & Biotechnology*, 19:215–225.
- Madigan, M. T., Martinko, J. M., and Parker, J. (2003). *Brock biology of microorganisms*. Prentice Hall, 10<sup>th</sup> edition.

- Manceau, A. (1995). The mechanism of anion adsorption on iron oxides: Evidence for the bonding of arsenate tetrahedra on free  $\text{Fe}(\text{O},\text{OH})_6$  edges. *Geochimica et Cosmochimica Acta*, 59:3647–3653.
- Mandal, B. K., Chowdhury, T. R., Samata, G., Mukherjee, D. P., Chanda, C. R., Saha, K. C., and Chankraborti, D. (1998). Impact of safe water for drinking and cooking on five arsenic-affected families for 2 years in West Bengal, India. *The Science of the Total Environment*, 218:185–201.
- Mandal, B. K. and Suzuki, K. T. (2002). Arsenic round the world: A review. *Talanta*, 58:201–235.
- Mann, S., Sparks, N. H. C., Couling, S. B., Larcombe, M. C., and Frankel, R. B. (1989). Crystallochemical characterization of magnetic spinels prepared from aqueous solution. *Journal of the Chemical Society Faraday Transactions I*, 85:3033–3044.
- Manning, B. A., Fendorf, S., and Goldberg, S. (1998). Surface structure and stability of arsenic(III) on goethite: Spectroscopic evidence for inner-sphere complexes. *Environmental Science & Technology*, 32:2383–2388.
- Masscheleyn, P. H., Delaune, R. D., and Patrick, W. H. J. (1991). Effect of redox potential and pH on arsenic speciation and solubility in a contaminated soil. *Environmental Science & Technology*, 25:1414–1429.
- McArthur, J. M., Ravenscroft, P., Safiulla, S., and Thirlwall, M. F. (2001). Arsenic in groundwater: Testing pollution mechanisms for sedimentary aquifers in Bangladesh. *Water Resources Research*, 37:109–117.
- Mehra, O. P. and Jackson, M. L. (1958). Iron oxide removal from soils and clays by a dithionite-citrate system buffered with sodium bicarbonate. *Clays and Clay Minerals*, pages 317–326.
- Nevin, K. P. and Lovley, D. R. (2000). Potential for nonenzymatic reduction of Fe(III) via electron shuttling in subsurface sediments. *Environmental Science & Technology*, 34:2472–2478.
- Nevin, K. P. and Lovley, D. R. (2002a). Mechanisms for accessing insoluble Fe(III) oxide during dissimilatory Fe(III) reduction by *Geotrix fermentans*. *Applied and Environmental Microbiology*, 68:2294–2299.
- Nevin, K. P. and Lovley, D. R. (2002b). Mechanisms for Fe(III) oxide reduction in sedimentary environments. *Geomicrobiology Journal*, 19:141–159.
- Newman, D. K. and Kolter, R. (2000). A role for excreted quinones in extracellular electron transfer. *Nature*, 405:94–97.
- Nickson, R. T., McArthur, J. M., Ravenscroft, P., Burgess, W. G., and Ahmed, K. M. (2000). Mechanism of arsenic release to groundwater, Bangladesh and West Bengal. *Applied Geochemistry*, 15:403–413.
- Ona-Nguema, G., Abdelmoula, M., Jorand, F., Benali, O., Gehin, A., Block, J., and Genin, J. R. (2002). Microbial reduction of lepidocrocite  $\gamma\text{-FeOOH}$  by *Shewanella putrefaciens*; the formation of green rust. *Hyperfine Interactions*, 139/140:231–237.
- Paige, C. R., Snodgrass, W. J., Nicholson, R. V., and Scharer, J. M. (1996). The crystallization of arsenate-contaminated iron hydroxide solids at high pH. *Water Environment Research*, 68:981–987.
- Paige, C. R., Snodgrass, W. J., Nicholson, R. V., and Scharer, J. M. (1997a). An

- arsenate effect on ferrihydrite dissolution kinetics under acidic oxic conditions. *Water Resources*, 31:2370–2382.
- Paige, C. R., Snodgrass, W. J., Nicholson, R. V., Scharer, J. M., and He, Q. H. (1997b). The effect of phosphate on the transformation of ferrihydrite into crystalline products in alkaline media. *Water, Air and Soil Pollution*, 97:397–412.
- Paige, C. R., Snodgrass, W. J., Nicholson, R. V., and Sharer, J. M. (1994). Release of arsenic from model wastewater treatment solids: A mechanism based on surface ligand exchange. *Water Pollution Research Journal*, 29:507–530.
- Parkhurst, D. L. and Appelo, C. A. J. (1999). *User's guide to PHREEQC (version 2) - a computer program for speciation, batch-reaction, one-dimensional transport, and inverse geochemical calculations*. U.S. Geological Survey. Water Resources Investigations Report 99-4259.
- Pedersen, H. D., Postma, D., and Jakobsen, R. (2006). Release of arsenic associated with the reduction and transformation of iron oxides. To be submitted to *Geochimica et Cosmochimica Acta*.
- Pedersen, H. D., Postma, D., Jakobsen, R., and Larsen, O. (2005). Fast transformation of iron oxyhydroxides by the catalytic action of aqueous Fe(II). *Geochimica et Cosmochimica Acta*, 69:3967–3977.
- Pierce, M. L. and Moore, C. B. (1982). Adsorption of arsenite and arsenate on amorphous iron hydroxide. *Water Research*, 16:1247–1253.
- Postma, D. (1993). The reactivity of iron oxides in sediments: A kinetic approach. *Geochimica et Cosmochimica Acta*, 57:5027–5034.
- Poulton, S. W. (2003). Sulfide oxidation and iron dissolution kinetics during the reaction of dissolved sulfide with ferrihydrite. *Chemical Geology*, 202:79–94.
- Poulton, S. W., Krom, M. D., and Raiswell, R. (2004). A revised scheme for the reactivity of iron (oxyhydr)oxide minerals towards dissolved sulfide. *Geochimica et Cosmochimica Acta*, 68:3703–3715.
- Rancourt, D. G., Fortin, D., Pichler, T., Thibault, P., Lamarche, G., Morris, R. V., and Mercier, H. J. (2001). Mineralogy of a natural As-rich hydrous ferric oxide coprecipitate formed by mixing of hydrothermal fluid and seawater: Implications regarding surface complication and color banding in ferrihydrite deposits. *American Mineralogist*, 86:834–851.
- Randall, S. R., Sherman, D. M., and Ragnarsdottir, K. V. (2001). Sorption of As(V) on green rust ( $\text{Fe}_4(\text{II})\text{Fe}_2(\text{III})(\text{OH})_{12}\text{SO}_4 \cdot 3\text{H}_2\text{O}$ ) and lepidocrocite ( $\gamma\text{-FeOOH}$ ): Surface complexes from EXAFS spectroscopy. *Geochimica et Cosmochimica Acta*, 65:1015–1023.
- Raven, K. P., Jain, A., and Loeppert, R. H. (1998). Arsenite and arsenate adsorption on ferrihydrite: Kinetics, equilibrium, and adsorption envelopes. *Environmental Science & Technology*, 32:344–349.
- Rea, B. A., Davis, J. A., and Waychunas, G. A. (1994). Studies of the reactivity of the ferrihydrite surface by iron isotopic exchange and Mössbauer spectroscopy. *Clays and Clay Minerals*, 42:23–34.
- Redman, A. D., Macalady, D. L., and Ahmann, D. (2002). Natural organic matter affects arsenic speciation and sorption onto hematite. *Environmental Science & Technology*, 23:2889–2896.

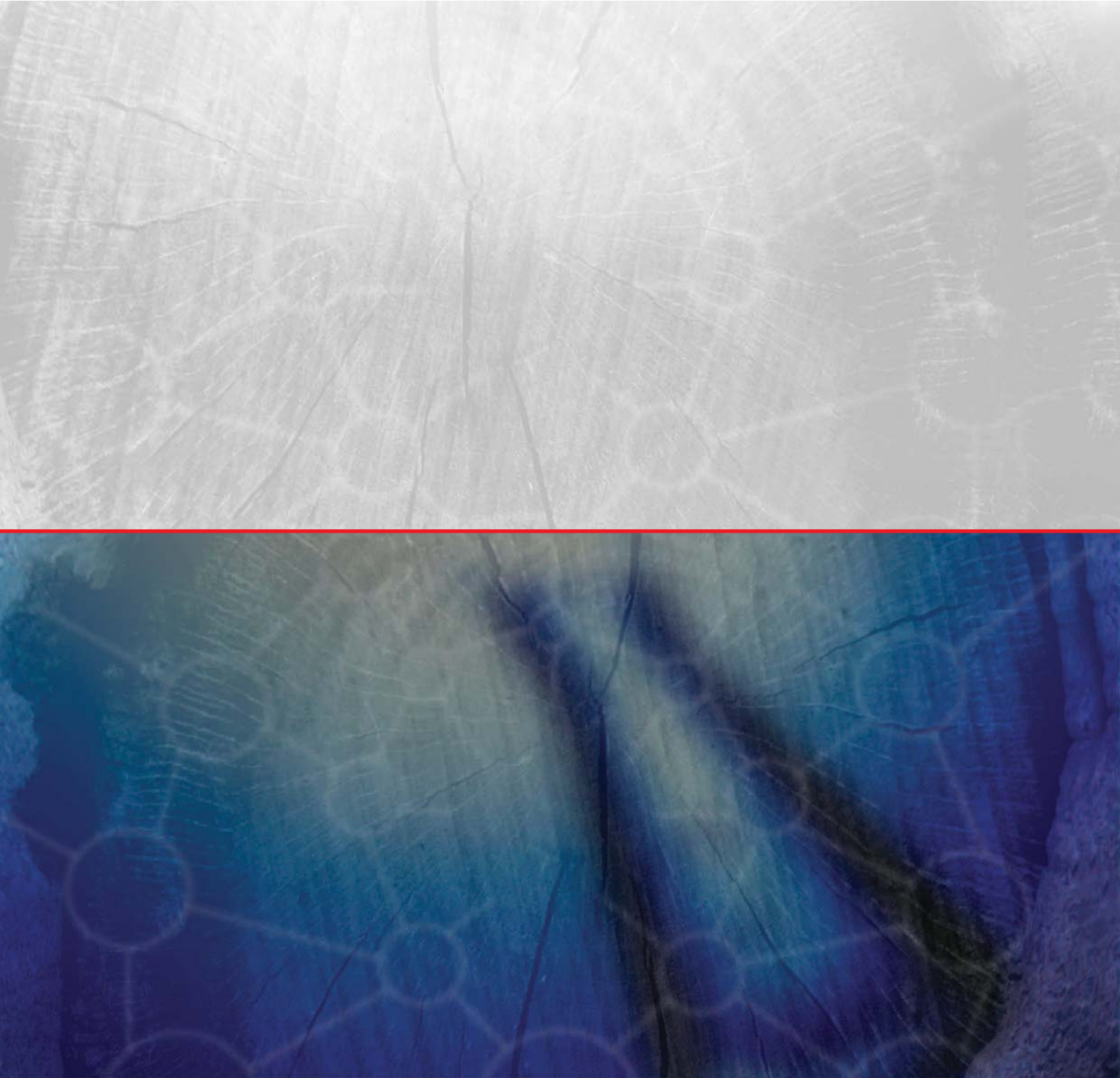


- Regenspurg, S., Gössner, A., Peiffer, S., and Küsel, K. (2002). Potential remobilization of toxic anions during reduction of arsenated and chromated schwertmannite by dissimilatory Fe(III)-reducing bacterium *Acidiphilium cryptum* JF-5. *Water, Air and Soil Pollution: Focus*, 2:57–67.
- Regenspurg, S. and Peiffer, S. (2005). Arsenate and chromate incorporation in schwertmannite. *Applied Geochemistry*, 20:1226–1239.
- Reguera, G., McCarthy, K. D., Mehta, T., Nicoll, J. S., Tuominen, M. T., and Lovley, D. R. (2005). Extracellular electron transfer via microbial nanowires. *Nature*, 435:1098–1101.
- Richmond, W. R., Loan, M., Morton, J., and Parkinson, G. M. (2004). Arsenic removal from aqueous solution via ferrihydrite crystallization control. *Environmental Science & Technology*, 38:2368–2372.
- Rimstidt, J. D. and Vaughan, D. J. (2003). Pyrite oxidation: A state-of-the-art assessment of the reaction mechanism. *Geochimica et Cosmochimica Acta*, 67:873–880.
- Roden, E. E. (2003a). Analysis of long-term bacterial vs. chemical Fe(III) oxides reduction kinetics. *Environmental Science & Technology*, 37:1319–1324.
- Roden, E. E. (2003b). Fe(III) oxide reactivity toward biological versus chemical reduction. *Environmental Science & Technology*, 37:1319–1324.
- Roden, E. E. and Lovley, D. R. (1993). Evaluation of  $^{55}\text{Fe}$  as a tracer of Fe(III) reduction in aquatic sediments. *Geomicrobiology Journal*, 11:49–56.
- Roden, E. E. and Zachara, J. M. (1996). Microbial reduction of crystalline iron(III) oxides: Influence of oxide surface area and potential for cell growth. *Environmental Science & Technology*, 30:1618–1628.
- Rozan, T. F., Taillefert, M., Trouwborst, R. E., Glazer, B. T., Ma, S., Herszage, J., Valdes, L. M., Price, K. S., and Luther, I. G. W. (2002). Iron-sulfur-phosphorus cycling in the sediments of a shallow coastal bay: Implications for sediment nutrient release and benthic macroalgal blooms. *Limnology and Oceanography*, 47:1346–1354.
- Schwartz, C. H., Blute, N. K., Badruzzaman, B., Ali, A., Brabander, D., Jay, J., Besancon, J., Islam, S., Hemond, H. F., and Harvey, C. F. (2004). Mobility of arsenic in a Bangladesh aquifer: Interference from geochemical profiles, leaching data, and mineralogical characterization. *Geochimica et Cosmochimica Acta*, 68:4539–4557.
- Schwertmann, U., Friedl, J., Stanjek, H., and Schulze, D. G. (2000). The effect of Al on Fe oxides. XIX Formation of As-substituted hematite from ferrihydrite at 25°C and pH 4 to 7. *Clays and Clay Minerals*, 48:159–172.
- Schwertmann, U. and Murad, E. (1983). Effect of pH on the formation of goethite and hematite from ferrihydrite. *Clays and Clay Minerals*, 31:277–284.
- Schwertmann, U. and Taylor, R. M. (1973). The in vitro transformation of soil lepidocrocite to goethite. *Pseudogley and gley Trans Comm V & VI Int Sci Soc*, 1971:45–54.
- Seeliger, S., Cord-Ruwisch, R., and Schink, B. (1998). A periplasmic and extracellular c-type cytochrome of *Geobacter sulfurreducens* acts as a ferric iron reductase and as an electron carrier to other acceptors or to partner bacteria. *Journal of Bacteriology*, 180:3686–3691.

- Sherman, D. M. (1987). Molecular orbital (SCF-X $\alpha$ -SW) theory of metal-metal charge transfer processes in minerals I. Application to Fe<sup>2+</sup>  $\rightarrow$  Fe<sup>3+</sup> charge transfer and 'electron delocalization' in mixed-valence iron oxides and silicates. *Physics and Chemistry of Minerals*, 14:355–363.
- Sherman, D. M. and Randall, S. R. (2003). Surface complexation of arsenic(V) to iron(III) (hydr)oxides: Structural mechanism from ab initio molecular geometrics and EXAFS spectroscopy. *Geochimica et Cosmochimica Acta*, 67:4223–4230.
- Smedley, P. L. and Kinniburgh, D. G. (2002). A review of the source, behaviour and distribution of arsenic in natural waters. *Applied Geochemistry*, 17:517–568.
- Sørensen, J. and Thorling, L. (1991). Stimulation by lepidocrocite ( $\gamma$ -FeOOH) of Fe(II)-dependent nitrite reduction. *Geochimica et Cosmochimica Acta*, 55:1289–1294.
- Straub, K., Benz, M., and Schink, B. (2001). Iron metabolism in anoxic environments at near neutral pH. *FEMS Microbiology Ecology*, 34:181–186.
- Stumm, W. (1992). *Chemistry of the solid-water interface: Processes at the mineral-water and particle-water interface in natural systems*, chapter Redox processes mediated by surfaces, pages 309–335. John Wiley & Sons, Inc.
- Stumm, W. (1995). The inner-sphere surface complex: A key to understanding surface reactivity. *American Chemical Society*, 244:1–32.
- Sudukar, C., Subbanna, G. N., and Kutta, T. R. N. (2003). Effect of anions on the phase stability of  $\gamma$ -FeOOH nanoparticles and the magnetic properties of gamma-ferric oxide derived from lepidocrocite. *Journal of Physics and Chemistry of Solids*, 64:2337–2349.
- Sulzberger, B., Suter, D., Siffert, C., Banwart, S., and Stumm, W. (1989). Dissolution of Fe(III)(hydr)oxides in natural waters; laboratory assesment on the kinetics controlled by surface coordination. *Marine Chemistry*, 28:127–144.
- Sun, T., Paige, C. R., and Snodgrass, W. J. (1999). Combined effect of arsenic and cadmium on the transformation of ferrihydrite into crystalline products. *Journal of University of Science and Technology Beijing*, 6:168–173.
- Sun, X. and Doner, H. E. (1996). An investigation of arsenate and arsenite bonding structures on goethite by FTIR. *Soil Science*, 161:865–872.
- Suter, D., Banwart, S., and Stumm, W. (1991). Dissolution of hydrous iron(III) oxides by reductive mechanisms. *Langmuir*, 7:809–813.
- Tamura, Y., Ito, K., and Katsura, T. (1983). Transformation of  $\gamma$ -FeO(OH) to Fe<sub>3</sub>O<sub>4</sub> by adsorption of iron(II) on  $\gamma$ -FeO(OH). *Journal of Chemical Society*, 1983:189–194.
- Tareq, S. M., Safiullah, S., Anawar, H. M., Rahman, M., and Ishizuka, T. (2004). Arsenic pollution in groundwater: A self-organizing complex geochemical process in the deltaic sedimentary environment, Bangladesh. *The Science of the Total Environment*, 313:213–226.
- Thamdrup, B. (2000). Bacterial manganese and iron reduction in aquatic sediments. *Advances in Microbial Ecology*, 16:41–84.
- Tronc, E., Belleville, P., Jolivet, J., and Livage, J. (1992). Transformation of ferric hydroxide into spinel by FeII adsorption. *Langmuir*, 8:313–319.
- Turick, C. E., Tisa, L. S., and Caccavo, F. J. (2002). Melanin production and use as a soluble electron shuttle for Fe(III) oxide reduction and as a terminal electron

- acceptor by *Shewanella alga* BrY. *Applied and Environmental Microbiology*, 68:2436–2444.
- Twidwell, L. G., Robins, R. G., and Hohn, J. W. (2005). *Arsenic Metallurgy*, chapter The removal of arsenic from aqueous solution by coprecipitation with iron(III), pages 3–24. TMS (The Minerals, Metals & Materials Society).
- van Geen, A., Rose, J., Thoraj, S., Garnier, J. M., Zheng, Y., and Bottero, J. Y. (2004). Decoupling of As and Fe release to Bangladesh groundwater under reducing conditions. Part II. Evidence from sediment incubations. *Geochimica et Cosmochimica Acta*, 68:3475–3486.
- van Oosterhout, G. W. (1967). The transformation of  $\gamma$ -FeO(OH) to  $\alpha$ -FeO(OH). *Journal of Inorganic and Nuclear Chemistry*, 29:1235–1238.
- Viraraghavan, T., Subramanian, K. S., and Aruldoss, J. A. (1999). Arsenic in drinking water - problems and solutions. *Water Science and Technology*, 40:69–76.
- Waychunas, G. A., Davis, J. A., and Fuller, C. C. (1995a). Geometry of sorbed arsenate of ferrihydrite and crystalline FeOOH: Re-evaluation of EXAFS results and topological factors in predicting sorbate geometry, and evidence for monodentate complexes. *Geochimica et Cosmochimica Acta*, 59:3655–3661.
- Waychunas, G. A., Fuller, C. C., Rea, B. A., and Davis, J. A. (1996). Wide angle X-ray scattering (WAXS) study of 'two-line' ferrihydrite structure: Effect of arsenate sorption and counterion variation and comparison with EXAFS results. *Geochimica et Cosmochimica Acta*, 60:1765–1781.
- Waychunas, G. A., Rea, B. A., Fuller, C. C., and Davis, J. A. (1993). Surface chemistry of ferrihydrite: Part 1. EXAFS studies of the geometry of coprecipitated and adsorbed arsenate. *Geochimica et Cosmochimica Acta*, 57:2251–2269.
- Waychunas, G. A., Xu, N., Fuller, C. C., Davis, J. A., and Bigham, J. M. (1995b). XAS study of  $\text{AsO}_4^{3-}$  and  $\text{SeO}_4^{2-}$  substituted schwertmannites. *Physica B*, 208 & 209:481–483.
- Wehrli, B., Sulzberger, B., and Stumm, W. (1989). Redox processes catalyzed by hydrous oxide surfaces. *Chemical Geology*, 78:167–179.
- Welham, N. J., Malatt, K. A., and Vukcevic, S. (2000). The stability of iron phases presently used for disposal from metallurgical systems - a review. *Minerals Engineering*, 13:911–931.
- Williams, A. G. B. and Scherer, M. M. (2004). Spectroscopic evidence for Fe(II)-Fe(III) electron transfer at the Fe oxide-water interface. *Environmental Science & Technology*, 38:4782–4790.
- Yao, W. and Millero, F. J. (1996). Oxidation of hydrogen sulfide by hydrous Fe(III) oxides in seawater. *Marine Chemistry*, 52:1–16.
- Zachara, J. M., Cowan, C. E., and Resch, C. T. (1991). Sorption of divalent metals on calcite. *Geochimica et Cosmochimica Acta*, 55:1549–1562.
- Zachara, J. M., Kukkadapu, R. K., Fredrickson, J. K., Gorby, Y. A., and Smith, S. C. (2002). Biomineralization of poorly crystalline Fe(III) oxides by dissimilatory metal reducing bacteria (DMRB). *Geomicrobiology Journal*, 19:179–207.
- Zinder, B., Furrer, G., and Stumm, W. (1986). The coordination chemistry of weathering: II. Dissolution of Fe(III) oxides. *Geochimica et Cosmochimica Acta*, 50:1861–1869.
- Zobrist, J., Dowdle, P. R., Davis, J. A., and Oremland, R. S. (2000). Mobilization of

arsenite by dissimilatory reduction of adsorbed arsenate. *Environmental Science & Technology*, 34:4747–4753.

A microscopic image of plant cells, showing a network of cell walls and circular cell structures. The image is split horizontally by a red line. The top half is in grayscale, and the bottom half is in color, showing shades of blue and purple.

**Institute of Environment & Resources**

Technical University of Denmark  
Bygningstorvet, Building 115  
DK-2800 Kgs. Lyngby

Phone: +45 4525 1600

Fax: +45 4593 2850

e-mail: [reception@er.dtu.dk](mailto:reception@er.dtu.dk)

Please visit our website [www.er.dtu.dk](http://www.er.dtu.dk)

ISBN 87-91855-03-9